applied sciences

MDPI

Article

Possible Approaches to Studying the Influence of Magnetic Fields and Mechanical Effects on the Physicochemical Properties of Aqueous IgG Colloids

Egor I. Nagaev [1,*], Elena A. Molkova [1], Vladimir I. Pustovoy [1], Tatyana A. Matveeva [1], Dmitry A. Zakharov [1], Alexander V. Simakin [1], Evgenia V. Stepanova [1], Natalia A. Semenova [1], Veronika E. Reut [2], Valery P. Kalinitchenko [3], Valery A. Kozlov [1,4] and Nikolai F. Bunkin [1,4]

[1] Prokhorov General Physics Institute of the Russian Academy of Sciences, 119991 Moscow, Russia; bronkos627@gmail.com (E.A.M.); pustovoy@nsc.gpi.ru (V.I.P.); pticek@yandex.ru (T.A.M.); zaharov121221@mail.ru (D.A.Z.); avsimakin@gmail.com (A.V.S.); jacky-st@yandex.ru (E.V.S.); natalia.86@inbox.ru (N.A.S.); v.kozlov@hotmail.com (V.A.K.); nbunkin@mail.ru (N.F.B.)
[2] Department of Biophysics, Belarusian State University, 220030 Minsk, Belarus; reutve@bsu.by
[3] Institute of Fertility of Soils of South Russia, 346493 Persianovka, Russia; kalinitch@mail.ru
[4] Department of Fundamental Sciences, Bauman Moscow State Technical University, 105005 Moscow, Russia
* Correspondence: nagaev_e@kapella.gpi.ru

Abstract: The influence of various mechanical influences (transfusion, stirring, vibration, shaking, etc.) and magnetic installations (used in the application of spin chemistry methods) on colloidal solutions of protein and water, which are often used in pharmaceutical production, was studied. It has been shown that when mechanical influences are applied, physical and chemical properties of water and aqueous colloids of the IgG protein are changed. Magnetic fields do not have a significant effect on water; however, variation in a number of physical and chemical characteristics is observed in protein colloids. Moreover, the effect after exposure to magnetic fields with a frequency of 8 Hz is higher compared to the effect after exposure to magnetic fields with a frequency of 50 Hz. This effect persists even at extremely low concentrations of IgG protein molecules. The measurement system proposed in this work makes it possible to monitor the state of protein molecules in a non-invasive mode. In the future, optical and potentiometric methods built into flow systems can be used at all stages of the production of protein pharmaceuticals.

Keywords: water; protein colloids; immunoglobulin G; magnetic fields; mechanical influences

Citation: Nagaev, E.I.; Molkova, E.A.; Pustovoy, V.I.; Matveeva, T.A.; Zakharov, D.A.; Simakin, A.V.; Stepanova, E.V.; Semenova, N.A.; Reut, V.E.; Kalinitchenko, V.P.; et al. Possible Approaches to Studying the Influence of Magnetic Fields and Mechanical Effects on the Physicochemical Properties of Aqueous IgG Colloids. *Appl. Sci.* **2023**, *13*, 13055. https://doi.org/10.3390/app132413055

Academic Editors: Mohsin Khurshid and Abdul Ahad

Received: 21 October 2023
Revised: 1 December 2023
Accepted: 5 December 2023
Published: 7 December 2023

1. Introduction

Protein-based drugs have been used in therapy for a long time. It is believed that the first purified protein used in medicine was the digestive enzyme pepsin. This happened shortly after the discovery of pepsin by T. Schwann in 1836 [1]. Almost two centuries have passed since then, and today medicine is increasingly using protein drugs in a wide variety of areas of clinical practice [2]. Enzyme-based protein preparations are the most widely used in medicine [3] and cosmetology [4]. Enzymes are mainly used 1. In medical diagnostic kits; 2. To eliminate enzyme deficiency in order to compensate for congenital or acquired functional deficiency; 3. For lysis of blood clots and removal of non-viable structures; 4. In the treatment of malignant neoplasms; 5. For detoxification, etc. [5]. In addition to enzymes, immunoglobulins (antibodies), protein-based vaccines, interferons, and regulatory proteins are used in medicine [6]. Separate mention should be made of protein poisons [7], including neurotoxic ones [8,9]. Protein-based drugs have a number of undeniable advantages. First, proteins can be specific targets for drugs and can themselves act on specific targets, which leads to minimization of side effects. Secondly, proteins can be used to replace or enhance natural proteins in the body, which leads to the correction and/or normalization of biological processes. Thirdly, proteins have great potential in the

field of personalized medicine, since molecular biology makes it possible to create protein molecules that best suit the individual needs and characteristics of the patient. It is already clear that in the future protein drugs will have many new opportunities and prospects in the field of medicine [10–13]. For example, a new class of pharmaceutical protein drugs based on gradual technology has recently emerged [14]. Gradual technology is based on the step-by-step processing of a pharmaceutical substance of a protein origin, at each stage of which its dilution is accompanied by controlled exposure using an automated microfluidic system. It is known that new physical properties of protein solutions can be detected after vibrational exposure during the preparation of the protein dilutions [15,16].

In the early stages, living organisms were the main source of proteins in medicine. Currently, recombinant protein drugs that are produced in bioreactors dominate [17]. The general method for obtaining a recombinant protein can be reduced to the following stages: 1. Molecular cloning of the gene; 2. Transformation of bacterial cells; 3. Selection of clones of super-producers; 4. Reproduction of clones; 5. Protein isolation; 6. Protein purification [18]. The main problem in this case is the problem of incorrect structural arrangement of protein chains in space and, as a result, the production of an inactive protein [19]. In some cases, up to 70% of the protein preparation has incorrect structural folding. Non-invasive monitoring of the structure of recombinant proteins at all technological stages will avoid unnecessary production losses.

Not all production facilities are built new for the production of protein preparations; the production of protein preparations is often integrated into existing technological lines. Most pharmaceutical production in the countries of the former Warsaw Pact has sources of mechanical vibrations (mixers, pumps, shakers) with frequencies of 4.4–12 Hz in their production lines. It has been known for almost a century that, under mechanical stress, the activity of protein molecules can significantly decrease [20] due to structural damage. Also, pharmaceutical production in the countries of the former Warsaw Pact often uses spin chemistry methods, namely magnetic fields with a frequency of 8–10 Hz. An integral part of all pharmaceutical production is also the alternating field of electrical networks with a frequency of 50 Hz [21]. The influence of changes in magnetic and hypomagnetic conditions on biological objects and molecules is discussed in detail in recent review works [22,23]. The purpose of this work is to develop methods for monitoring the state of protein preparations when using technological lines of existing production facilities.

It is shown that using general laboratory methods (optical and potentiometric control) and partially rheometry allows us to obtain the information about protein molecules' state in solutions with IgG concentrations from 1 mg/mL. The influence of the most commonly used mechanical influences and the effects of magnetic fields on the physical and chemical properties of protein solutions have been studied. The influence of the impacts used in technological lines on the properties of protein solutions obtained using gradual technology has been studied. It has been established that magnetic fields and mechanical influences lead to modifications of physical and chemical properties of aqueous immunoglobulin G colloids. The proposed measurement system makes it possible to monitor the state of protein molecules in a non-invasive mode.

2. Materials and Methods

2.1. Aqueous Immunoglobulin G Colloids

In this study, normal human immunoglobulin G (IgG) solutions (Microgen, Moscow, Russia) with IgG concentration of 100 mg/mL were used. To prepare experimental samples, initial solutions were dissolved in deionized water (18 Mom × cm).

2.2. Potentiometric Measurements

For potentiometric measurements, we used the SevenExcellence pH meterS 400 laboratory complex (Mettler Toledo, Zürich, Switzerland) with electrodes for measuring pH InLab Expert Pro-ISM, redox potential InLab RedOx (all Mettler Toledo, Zürich, Switzerland). To measure the specific conductivity of liquids, a SevenExcellence Cond meterS

700 conductivity meter with an InLab 731-ISM electrode (Mettler Toledo, Zürich, Switzerland) was used. To measure the concentration of molecular oxygen, a Seven2Go pro S9 DO meter (Mettler Toledo, Zürich, Switzerland) was used. All measurements were carried out in the thickness of the liquid with laminar mixing of the liquid at a speed of 60–100 rpm. After each measurement, the electrodes were washed with deionized water until completely clean, which was monitored using standard deionized water readings. Details of the methods have been described previously [24,25].

2.3. Optical Methods

To obtain the information about refractive indexes of protein solutions, automatic multiwavelength refractometer Abbemat MW (Anton Paar, Graz, Austria) was used. Parameters of the experiments are as follows: sample volume—1 mL, temperature—25 °C, wavelength—632.9 nm.

Absorption spectra measurements were obtained using two-beam spectrophotometer Cintra 4040 (GBS Scientific Equipment Pty Ltd., Melbourne, VIC, Australia). Experiments were carried out at room temperature (~22 °C). Quartz cuvettes with an optical path of 10 mm were used for control and experimental solutions.

Three-dimensional fluorescent maps were obtained using an FP-8300 spectrofluorimeter (Jasco Applied Sciences, Dartmouth, NS, Canada). 10 × 10 mm Quartz cuvettes (Jasco Applied Sciences, Dartmouth, Canada) were used for these measurements. Experiments were carried out at room temperature (~22 °C). A standard measurement regime was used, details of which are described in [26]. Two-dimensional fluorescence spectra were measured at an excitation wavelength of 280 nm.

Hydrodynamic diameters of molecules in solutions were measured using Zetasizer Ultra Red Label (Malvern Panalytical Ltd., Malvern, UK). Standard polystyrene cuvettes (DTS0012) were used for these experiments. Experiments were carried out at 25 °C. Size distributions were calculated with Malvern ZS Xplorer software (version 2.0.1.1) [27].

2.4. Ultrasonic Spectroscopy

Ultrasonic spectroscopy evaluates the speed of passage of acoustic waves through the control and test samples. This method enables estimating the amount of water entering the hydration shell of the macromolecule: the hydration number, which allows one to evaluate the conformational state of the macromolecule. The measurement principle is as follows: liquid samples (control and experimental) with a volume of 1 mL are placed in their own compartment, in each of which two plane-parallel piezoceramic plates are fixed at the edges, performing the function of electro-acoustic transducers. Two harmonic signals are used: the first signal with a 6–8 MHz frequency is applied to one of the plates, and the other signal with resonances is taken from the other plate, the characteristics of which depend on the material of the cell and on the properties of the sample being measured. Many quantities are measured (number of peaks, frequency, and width) among which one resonant peak is automatically selected for the control and test sample, and at the output of the device, the ratio of the frequencies of this peak from the measuring and reference cuvette is given. The magnitude of this frequency ratio depends, first of all, on the density of the solution. The temperature during these experiments was 25 °C, which was recorded in two cuvettes with an accuracy of 0.01 °C. Details of the method have been described previously [28].

2.5. Dynamic Viscosity Measurement

Dynamic viscosity measurements were carried out using a SmartPave 102 rheometer (Anton Paar GmbH, Graz, Austria). The dynamic viscosity of the aqueous solutions was measured at 25 °C. The shear rates during the experiments varied from 100 s^{-1} to 1000 s^{-1}. A DG26.7 measurement set was used in these experiments. We worked in the dry heating mode, in which there is no water flow around the sample. The sample volume was 3.8 mL.

A data analysis was performed using RheoCompass™ software, version 1.30 (Anton Paar GmbH, Austria). Details of the method have been described previously [29].

2.6. Mechanical Vibration Effect

When conducting experiments, influences similar to those used on technological lines of pharmaceutical production were used. A special device was developed for implementing mechanical effects with different frequencies and amplitudes on samples (mixing in a turbulent flow in the vertical direction), described in detail in [30]. A vertical drilling machine, PBD 40 (Bosch, Gerlingen, Germany), with a lever for performing vertical vibrations was used as the basis of the device. Two modes of vibration impacts were used with the following characteristics: an amplitude of 20 mm with a frequency of 4.4 Hz (acceleration: 0.8 m/s^2) and an amplitude of 20 mm with a frequency of 12 Hz (acceleration: 2.7 m/s^2).

2.7. Exposure to Magnetic Fields

When conducting experiments, influences similar to those used on technological lines of pharmaceutical production were used. The 3-axis installation for exposure to magnetic fields was used in these experiments. The installation consists of three pairs of coils located perpendicular to each other. The size of the largest pair of coils is 85 cm. The installation includes the MP sensor FGM3D/100 (Sensys GmbH, Bad Saarow, Germany), an electronic field control unit, amplifiers, ADC/DAC USB-6343 (National Instruments, Ostin, TX, USA) for connecting the installation with a computer, and software. The system can create constant and alternating magnetic fields inside with induction from −60 to 60 μT. The inhomogeneity of the magnetic field in the center of the installation (a cube with a side of 5 cm) does not exceed 0.5%. The system is designed in such a way that it can compensate external magnetic field fluctuations: the compensation rate is more than 103 at a 1 Hz frequency, and at a frequency of 50 Hz, the compensation is approximately 40 times. The following modes were used in the work:

- Vertical axis: alternating magnetic field induction of 55 μT at a frequency of 8 Hz, and a constant MF of 0 μT (residual field < 20 nT). All other axes are 0 μT, both in constant MF and in alternating.
- Vertical axis: alternating magnetic field induction of 55 μT at a frequency of 50 Hz, and a constant MF of 0 μT. All other axes are 0 μT, both in constant MF and in alternating.

2.8. Statistic Calculations

Origin 2021, SigmaPlot 11.0, and GraphPad Prism 9.5.1. programs were used to analyze experimental data. Data from at least six independent experiments were used for averaging. Results are shown as mean values with standard deviations or means with standard errors. At least six measurements were used.

3. Results and Discussion

3.1. Study of the Physicochemical Properties of Aqueous IgG Colloid of Different Concentrations

Absorption spectra of aqueous IgG solutions are shown in Figure 1a as a function of concentration. The wavelengths attributed to local minima and maxima are as follows: 250 nm and 280 nm, 285 nm. It has been established that detailed optical absorption spectra are observed at a minimum concentration of IgG molecules of 0.1 mg/mL. The spectrum still remains characteristic at IgG concentration of 0.01 mg/mL. It is shown that when protein concentration is 0.001 mg/mL, the peak that corresponds to aminoacidic residues (280 nm) is no longer observed. The optical density of IgG solutions is minimal in the wavelength range 310–800 nm, but the optical density increases with increasing concentration of IgG molecules. It is known that the molecules of most proteins, including antibodies, do not absorb in the wavelength region 450–800 nm [31]. Typically, changes in optical density in such wavelengths are associated with light scattering rather than absorption [32], which in turn is associated with either denaturation of molecules or their aggregation [33]. To answer this question, the change in the hydrodynamic diameter of

light scatterers in aqueous IgG colloids with concentrations of 0.01–10 mg/mL was studied using the DLS method.

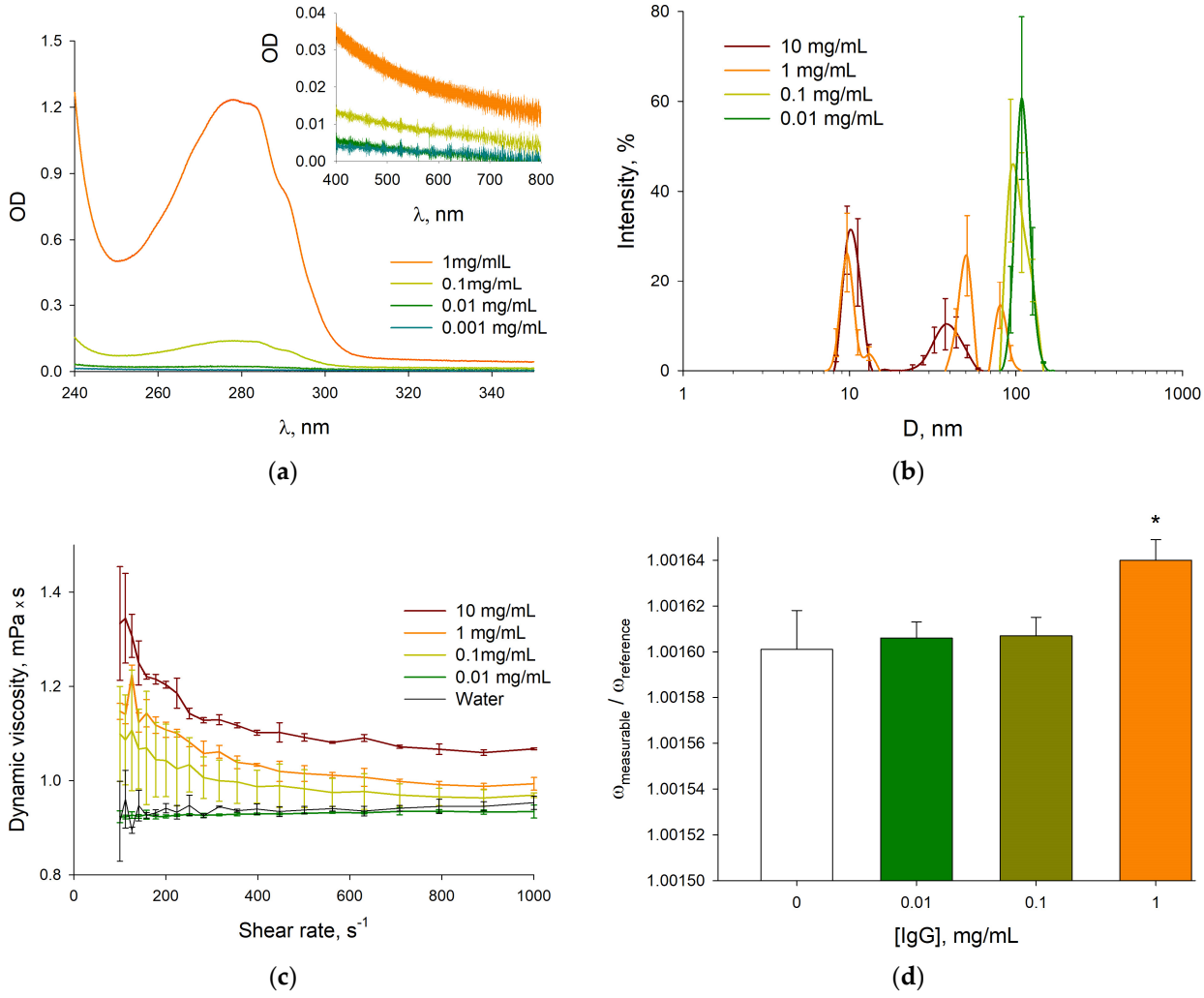

Figure 1. Changes in the physical and chemical properties of an aqueous colloid depending on the concentration of IgG. (**a**) Optical density changes of IgG solutions depending on the concentration of IgG. Internal figure shows the optical absorption in the wavelength range 400–800 nm. (**b**) Measurement with DLS method of the hydrodynamic diameter of light scatterers (IgG solutions) (concentrations: 0.01–10 mg/mL). (**c**) Changes in dynamic viscosity of aqueous IgG colloids with different content of antibodies at different shear stresses (M ± SD, n = 6). (**d**) Study of the frequency ratio in a measuring cell with an aqueous IgG colloid (concentration: 0.01–1 mg/mL) and a reference cell with water using ultrasonic spectroscopy (M ± SD, n = 6). *—statistical difference relative to samples not containing protein (*t*-test, $p < 0.05$).

Figure 1b shows measurements of the hydrodynamic particle diameter in a protein colloid containing different concentrations of IgG molecules. It has been shown that using the DLS method, in colloids with protein concentrations of 1 and 10 mg/mL, particles with a hydrodynamic diameter of ~10 nm are observed, corresponding in size to individual IgG molecules (immunoglobulin G molecules have sizes of about 10 nm (15 × 8 × 4 nm) [34]. Also, a fraction of 30–50 nm is observed in the size distribution; these are probably antibody aggregates. When the protein concentration is reduced to 0.1 and 0.01 mg/mL, no peak associated with individual antibody molecules is observed in the size distribution. This detects a fraction with sizes of 100–200 nm. Obviously, individual IgG molecules do not disappear. At low concentrations, scattering from individual molecules is a "mask" by

larger objects. To illustrate this thesis, we repeated the experiment with measuring the size of immunoglobulin, but in this case, to reduce the number of aggregates, the protein colloid was filtered using a membrane filter with an average pore size of 200 nm. The intensity particle size distribution results and autocorrelation functions for these measurements are presented in Appendix A (Figure A1). It is well-known that the intensity of light scattering from this fraction is several orders of magnitude less than from any fraction in a colloid containing 10 mg/mL protein. There are no light scatterers in freshly distilled water. Usually, the experiments used water that had been in contact with atmospheric gases for quite a long time. In such water, there are peaks in the region of 150–200 nm, with low light scattering intensity. It was previously shown that with prolonged contact of freshly distilled water with atmospheric gases, the water becomes saturated with oxygen and nitrogen molecules [35]. In this case, nano-sized clusters of gases, so-called bubstons, are formed in water [36]. The characteristic size of bubstons was determined earlier and is equal to 100–200 nm [37]. It can be assumed that the observed scatterers are most likely bubbles of dissolved gases—bubstons.

It is obvious that when the size distribution of objects in a colloid changes, a change in many physicochemical properties of the solution should be observed. Figure 1c shows the dynamic viscosity of IgG colloids at different concentrations at different shear stresses. It is shown that the dynamic viscosity of a protein solution increases at low shear stresses, which indicates that the protein colloid is a non-Newtonian fluid. The dynamic viscosity of solutions with IgG concentration of 0.01 mg/mL is close to deionized water viscosity, and the minimum detectable concentration is ~0.1 mg/mL. This observation is in good agreement with known data; it was previously shown that the minimum IgG concentration detectable with viscometry is ~0.1 mg/mL [38]. It should be noted that the viscosity of colloids depends not only on concentration, but also on temperature [39], pH [40], ionic strength, cation–anion environment [41], and the like [42–44]. Progress in viscometry research can be found in a literature review [45].

Colloidal protein solutions are characterized by pseudoelasticity, a decrease in dynamic viscosity with increasing shear stress [46]. In our experiments, pseudoelasticity was also observed. Additionally, it should be noted that the tabulated value for water, 0.87 mPa × s (25 °C), which does not depend on shear stress (Newtonian fluid), is not very different, but differs from what we measured. Water viscosity measurements in a rheometer can vary from 0.87 mPa × s to 0.94 mPa × s. Dynamic viscosity measurements are highly dependent on the geometry and volumes of the rotor and stator, especially when miniature attachments are used [47]. In such systems, there is a decrease in the absolute accuracy of measurements, while there is another significant advantage—a small volume—which is more important for measuring expensive protein solutions.

To assess the density of solutions, aqueous antibody colloids were studied using differential ultrasonic spectroscopy. Figure 1d shows the relationship between the resonant frequencies of the measuring and reference cuvettes. It is shown that only when the concentration of IgG in the aqueous solution is 1 mg/mL or more are significant differences detected with the ultrasonic spectroscopy.

Refractive indexes (RIs) of aqueous IgG colloids are shown in Figure 2a. Refractive index measurements of aqueous IgG solutions are shown in Figure 2a. It was shown that the RI of water and an aqueous colloid of antibodies (10 mg/mL) differs by more than 10^{-3} RI. Differences compared to the control are observed in aqueous antibody colloids with a concentration of 0.1 mg/mL or more. A summary plot on a logarithmic scale, with the solvent contribution subtracted, is presented in Figure 2b. An increment of 0.19 g/mL is set aside as a "theory". This increment is typical for most proteins and varies slightly depending on their amino acid composition [48]. The graph shows that almost the entire curve for IgG dissolved in water lies below the increment line of 0.19 g/mL, which may, for example, indicate that the IgG molecules are poorly dissolved in water. There may be another explanation for the results obtained. For example, a discrepancy with theory may be caused by other factors: changes in the hydration shell of IgG or differences in

the protein increment for a solvent from 0.19 g/mL. Previously, in [49], the relation of the increment of the RI of lysozyme in dependence with the chosen buffer was shown. The increment changes in the study had a wide range of variation from 0.153 to 0.272 depending on the buffer used. In general, the discrepancy between experimental data and theory requires further and more careful study.

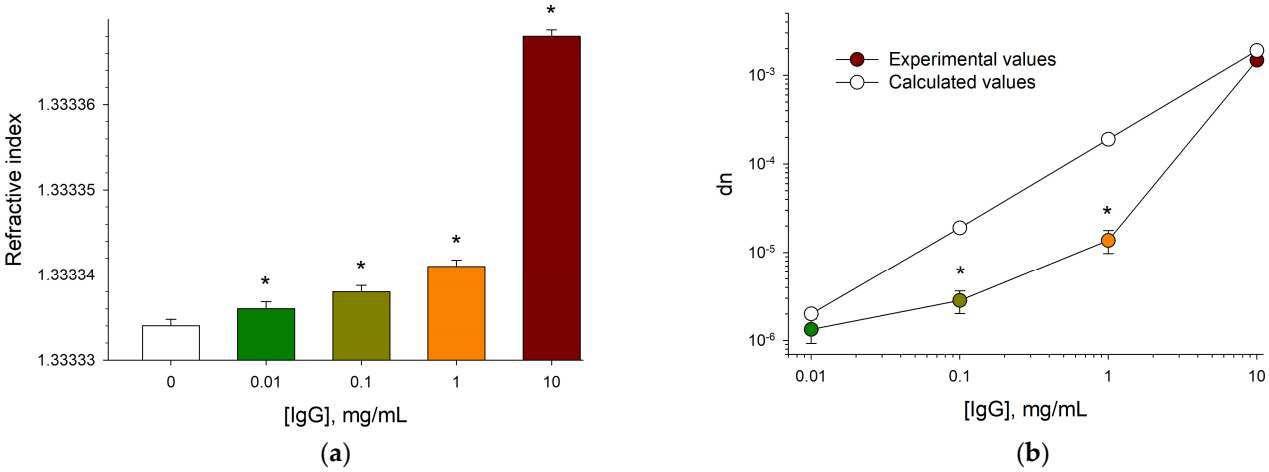

Figure 2. Refractive index of aqueous colloid as a function of IgG concentration. (**a**) Refractive index of IgG colloids with protein concentrations of 0.0001–0.1 mg/mL measured at a wavelength of 632.9 nm (M ± SD, n = 6). (**b**) Differential refractive indexes of different samples relative to the solvent according to the data from Figure 3a. An increment of 0.19 g/mL is set aside as a "theory". *—statistically significant difference relative to samples not containing protein (*t*-test, $p < 0.05$).

The specific conductivity of water and aqueous IgG protein colloids is shown in Figure 3a. It has been shown that the conductivity of protein colloids (IgG concentration < 1 mg/mL) does not differ much from the conductivity of water. The significant increase in specific electrical conductivity of solutions is observed at IgG concentration of 10 mg/mL.

Figure 3b shows the molecular oxygen content of water and aqueous colloids with different protein concentrations. It has been shown that significant differences in dissolved oxygen are visible only at the protein concentration of 10 mg/mL. Possibly, when the concentration of IgG is significantly high, the process of binding molecular oxygen with polar, positively charged amino acids in the protein (lysine, arginine, histidine) becomes noticeable. An alternative explanation is the displacement of gas molecules from water by dissolved molecules [50].

Figure 3c shows the redox potential values of water and aqueous colloids with different protein concentrations. At different concentrations of protein molecules, the values of the redox potential are observed, both higher and lower compared to the values of the control water. Multidirectional concentration trends can be explained by different surface charges of proteins. For IgG colloid, a "bell-shaped" dependence on protein concentration is observed. This form is most likely due to the fact that with increasing concentration, the protein passes the isoelectric point, which for IgG corresponds to pH ≈ 7.0 [51]. Therefore, for "small" concentrations, the protein surface is positively charged, and for "high" concentrations, it is negatively charged. Although the differences are visible to the naked eye, the large dispersion of data characteristic of this method makes it possible to distinguish between water and a 0.1 mg/mL IgG solution. Obviously, to confirm the assumption made about the influence of pH on the values of the redox potential, it is necessary to measure the impact of the concentration of IgG molecules on the pH values of the aqueous IgG colloid. Figure 3d shows the pH changes in water and in aqueous protein colloids. It has been shown that with increasing concentration of IgG in an aqueous colloid, the pH value increases. In the range of protein concentrations of 1–10 mg/mL, the pH value becomes more than 6.5; that is, the protein colloid passes the isoelectric point.

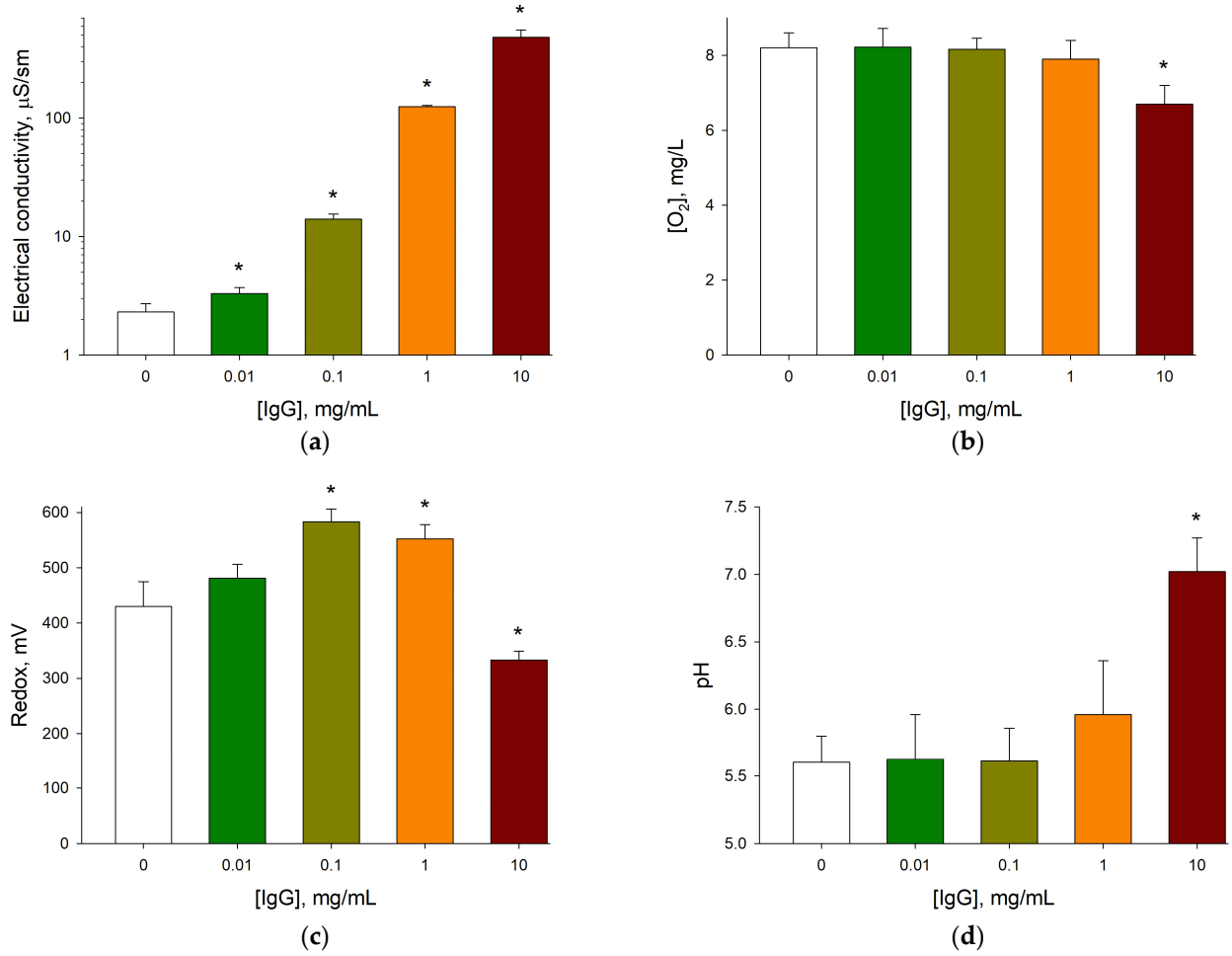

Figure 3. Changes in specific electrical conductivity (**a**), molecular oxygen concentration (**b**), oxidation–reduction potential (**c**), and pH (**d**) of an aqueous colloid depending on the concentration of IgG protein molecules (M ± SD, n = 6). *—statistically significant differences relative to samples not containing protein (*t*-test, $p < 0.05$).

Normalized 3D fluorescence spectra of aqueous solutions with different IgG concentration are shown in Figure 4. It has been shown that the protein is reliably detected in an aqueous colloidal solution up to concentrations of 10^{-4} mg/mL. In this case, it is recorded as fluorescence (~λ_{ex} = 280 nm, ~λ_{em} = 330 nm) caused by aromatic amino acid residues.

Thus, it has been established that most simple general laboratory methods can clearly distinguish between water and an aqueous colloid of antibodies with a concentration of at least 0.1–1.0 mg/mL; the only exception to the rule is fluorescence. Since the manuscript is devoted to the research of methods for control of quality of protein drugs in aqueous colloids, it was necessary to establish the possible influence of third-party physical influences present in pharmaceutical production. Today, in pharmaceutical production, various mechanical impacts are quite often used (transfusion, stirring, vibration, shaking, etc.) [52]. We conducted a literature study and found that the most common mechanical impacts are impacts with frequencies of about 4.4 and 12 Hz. Also, modern spin chemistry methods are often used in production [21]. Installations for spin-chemical reactions that allow exposing samples to weak alternating magnetic fields usually have frequencies of the order of 8–10 Hz (frequency close to the main Schumann resonance) [53], and an integral part of the background is an alternating field with a frequency of 50 Hz, characteristic of electrical networks.

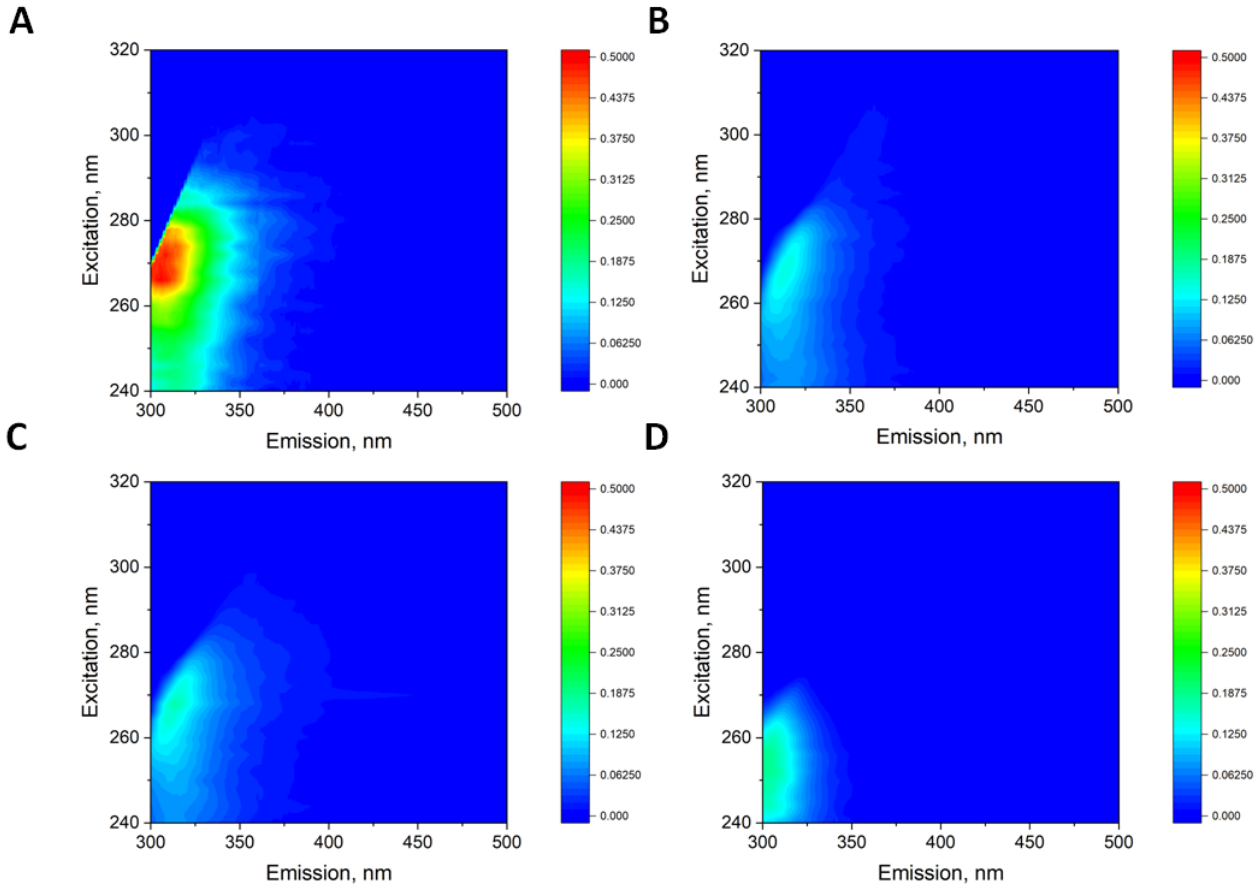

Figure 4. Three-dimensional fluorescence spectra of IgG protein after excitation at a wavelength of 240–320 nm, at different protein concentrations (mg/mL). (**A**)—10^{-4}, (**B**)—10^{-6}, (**C**)—10^{-8}, (**D**)—0.

3.2. Influence of Magnetic Field and Mechanical Action on the Physicochemical Properties of Aqueous IgG Colloids

The change in the optical density of an aqueous colloid with an IgG antibody concentration of 1 mg/mL was studied after external alternating magnetic field exposure with frequencies of 8 and 50 Hz, as well as mechanical stirring with frequencies of 4.4 and 12 Hz (Figure 5a). It has been shown that the shape of the curves characterizing optical absorption remains unchanged under all influences. There is no mixing of the maxima or minima of the curves. This allows us to assert that no significant destructive processes or intense chemical reactions occur in an aqueous colloid [54]. At wavelengths greater than 330 nm, there is no significant increase in optical absorption. An increase in optical absorption in aqueous protein colloids in the longer wavelength region of the visible range is usually associated with intense processes of denaturation or aggregation [55]. In this case, the spectra differ in intensity at the optical absorption peak (~280–290 nm). It should be noted that in the graph, the standard deviation is shown only upward in order to avoid overlapping curves. It has been shown that statistically significant differences are observed only between groups that were inside the setup with a magnetic field with frequencies of 8 and 50 Hz.

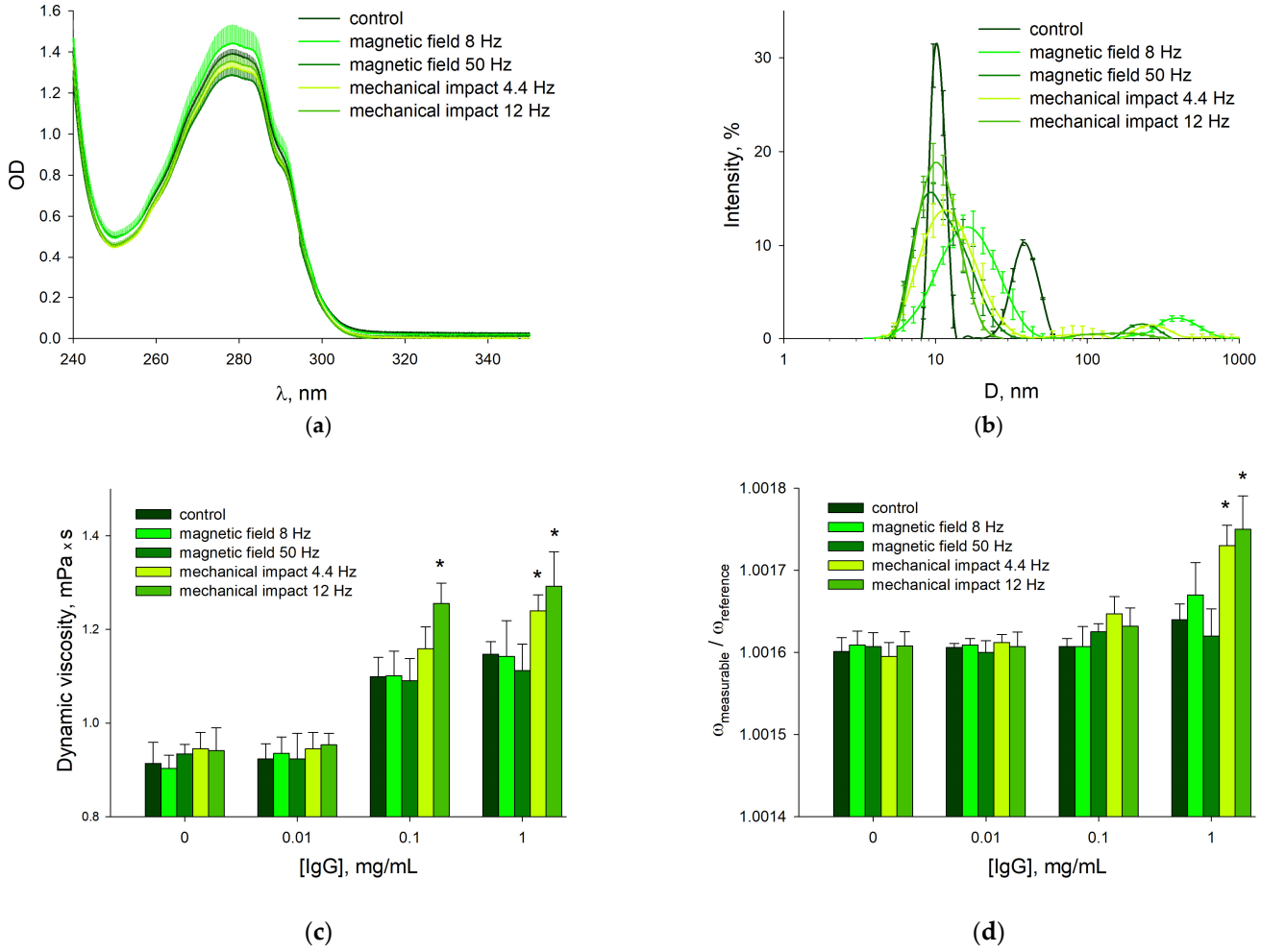

Figure 5. Physical and chemical characteristics of IgG solutions after exposure to an external magnetic field with frequencies of 8 and 50 Hz, as well as mechanical stirring with frequencies of 4.4 and 12 Hz (M ± SD, n = 6). (**a**) Change in the optical density of an aqueous colloid with an IgG concentration of 1 mg/mL after physical exposure (errors for SD are depicted only upward in order to avoid overlapping of the curves). (**b**) DLS measurement of the hydrodynamic diameter of light scatterers in solutions with IgG concentration of 10 mg/mL. (**c**) Change in dynamic viscosity of protein solutions with different concentrations of IgG at shear stresses of 100 s^{-1}. (**d**) Study of the frequency ratio in a measuring cell with an aqueous IgG colloid (concentration: 0.01–1 mg/mL) and a reference cell with water using ultrasonic spectroscopy. *—statistically significant differences relative to unexposed samples (*t*-test, $p < 0.05$).

DLS measurements of hydrodynamic diameters in aqueous IgG solutions with protein concentration of 10 mg/mL are shown in Figure 5b. It has been shown that in aqueous colloids with IgG concentration of 10 mg/mL, particles with a size of ~10 nm are observed, corresponding to individual protein molecules. In addition, a fraction with a hydrodynamic diameter of 30–50 nm is detected, corresponding to small antibody aggregates, and consisting of 30–60 protein molecules. Using the formula for the relationship between hydrodynamic radii and light scattering intensities [56], one can easily calculate that there are about 1500 individual molecules per aggregate in the colloid. Thus, we established that ~3% of protein molecules are located in aggregates. This explains why no pronounced scattering is observed in the absorption spectrum in the long-wave region of the visible range. The shape of the size distribution changes when the aqueous protein colloid is exposed to an alternating magnetic field (8 Hz). The average size increases to 18 nm, and a significant broadening of the peak is observed. This broadening is probably explained by

the presence in the colloid of significant quantities of not only individual protein molecules, but also dimers, trimers, and larger aggregates. Aggregates with an average size of about 400 nm, consisting of approximately 5×10^4 protein molecules, have also been recorded. There are about 10^5–10^6 individual molecules per aggregate in the colloid. The shape of the size distribution changes less significantly when the aqueous protein colloid is exposed to an alternating magnetic field (50 Hz). The average size does not change, although a significant broadening of the peak is observed. Aggregates with an average size of about 200 nm, consisting of approximately 6×10^3 protein molecules, have also been recorded. There are more than 106 individual molecules per aggregate in a colloid. When an aqueous protein colloid is exposed to mechanical mixing at frequencies of 4.4 and 12 Hz, the size distribution does not change significantly. The average size does not change, although some broadening of the peak is observed. A significant change in the size distribution can be considered in the absence of a significant number of aggregates in the diameter range 50–1000 nm. In other words, mechanical stirring can lead to disaggregation of protein aggregates with a hydrodynamic diameter of 30–50 nm. Obviously, the destruction of protein aggregates should lead to increasing viscosity of the aqueous colloid [57].

The impact of an alternating magnetic field with frequencies of 8 and 50 Hz, as well as mechanical stirring with frequencies of 4.4 and 12 Hz, on the change in the dynamic viscosity of IgG colloids is 0.01–1 mg/mL at a shear stress of 100 s^{-1} (Figure 5c). These shear stresses were chosen because they showed the greatest differences between groups of colloids with different protein concentrations. It was shown that statistical differences under the influence of physical factors were recorded only at protein concentrations of 0.1–1 mg/mL and only under mechanical influence. It should be noted that the differences in dynamic viscosity did not exceed 20%. In this case, magnetic fields did not affect the viscosity of protein colloids. It is probably these qualities of protein colloids that make it possible to use Brownian relaxation for immunoassays [58]. Today, magnetization harmonics, induced with a small low-frequency oscillating magnetic field, are actively used to obtain quantitative information about the microenvironment of magnetic nanoparticles coated with antibodies [59].

Using differential ultrasonic spectroscopy, the impact of a magnetic field with frequencies of 8 and 50 Hz, as well as mechanical stirring with frequencies of 4.4 and 12 Hz, was studied on the properties of an aqueous colloid of IgG antibodies with concentrations from 0.01 to 1 mg/mL (Figure 5d). It has been established that the studied effects do not lead to essential variation in the ratio of resonant frequencies in the measuring cell and the comparison cell. It was shown that statistical differences under the influence of physical factors were recorded only at protein concentrations of 1 mg/mL and only under mechanical influence. It should be noted that the differences in the frequency ratio characterizing the speed of sound in the colloid did not exceed 0.3%. It is known that this relationship characterizes the change in adiabatic elasticity and/or density of the medium [60]. From Figure 5b, it can be assumed that the density associated with dynamic viscosity changes predominantly, while the adiabatic elasticity of the medium should not change significantly.

The impact of an external magnetic field with frequencies of 8 and 50 Hz, as well as mechanical stirring with frequencies of 4.4 and 12 Hz, on the specific electrical conductivity of an aqueous colloid of IgG protein was investigated (Figure 6a). The specific electrical conductivity of H_2O and the aqueous protein colloid changes under the action of mechanical mixing with frequencies of 4.4 and 12 Hz. Fundamentally, this is not a priority result, since an increase in the electrical conductivity of H_2O and aqueous solutions after exposure to mechanical stirring was shown previously [61]. It should be noted that the conductivity of water under mechanical action increases by almost 50%, while under the action of mechanical shaking on protein colloids, the conductivity of H_2O increases only by 10–20%. It was previously assumed that an increase in the specific electrical conductivity of H_2O under mechanical action is associated with the formation of reactive oxygen species (ROS) [62,63]. It is believed that the generation of reactive oxygen species begins with the activation of O_2 dissolved in H_2O [64]. Briefly, the chain of chemical transformations

probably looks like this: an oxygen molecule is activated, goes into the singlet state, and attaches an electron, which leads to the formation of a superoxide anion radical. Under normal conditions, superoxide anion radicals are immediately protonated, which leads to the hydroperoxide radical formation, the dismutation of which produces H_2O_2 and O_2 (in the singlet state at 25%) [65,66]. There is an alternative point of view, according to which the water molecule undergoes dissociation into a hydroxyl radical, a proton, and an electron [67]. In this regard, it is important to investigate the influence of the applied physical influences on the concentration of O_2 in the liquid phase of H_2O and protein colloids.

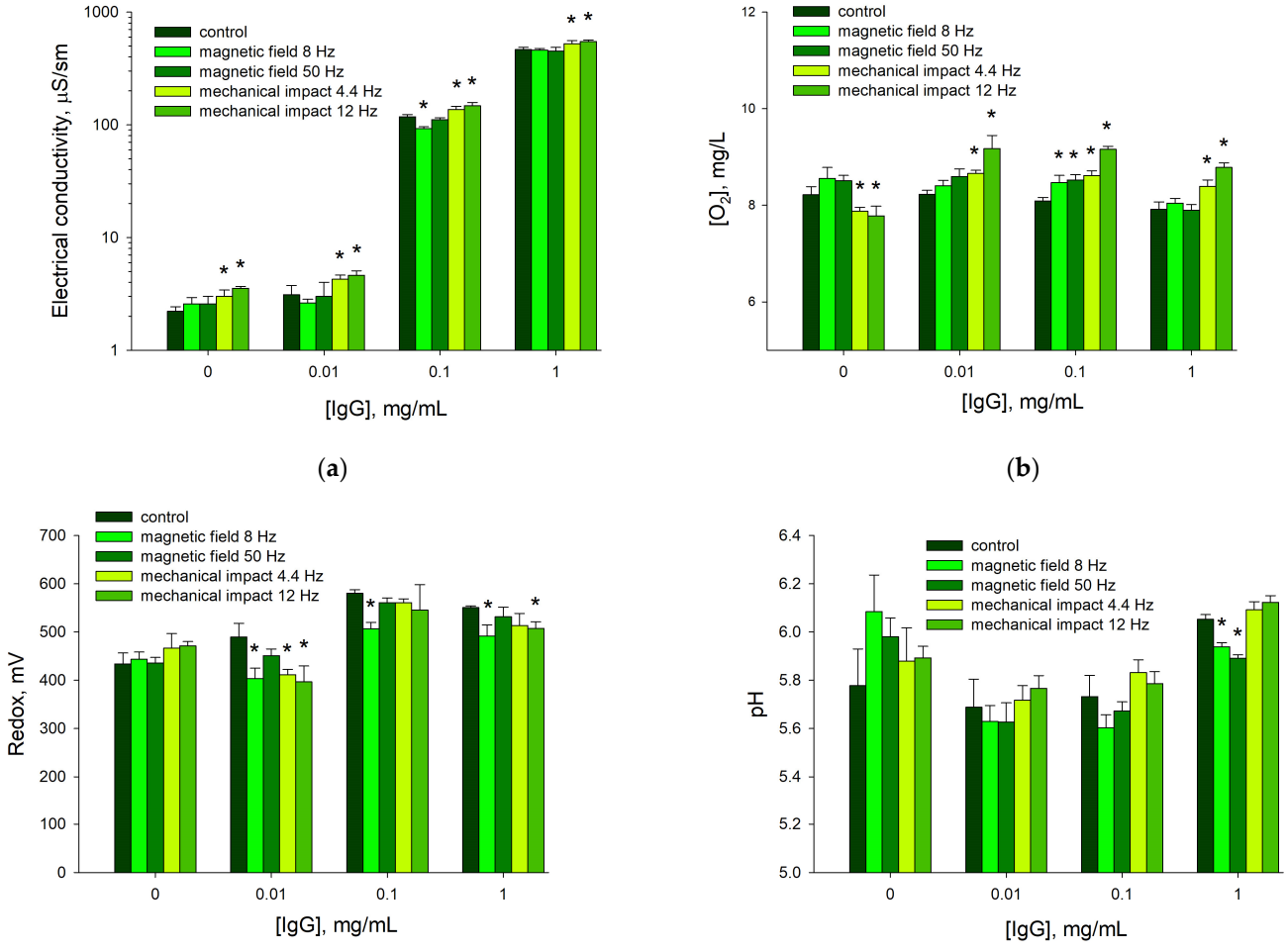

Figure 6. Changes in specific electrical conductivity (**a**), molecular oxygen concentration (**b**), redox potential (**c**), and pH (**d**) of aqueous colloid of IgG protein molecules after exposure to alternating magnetic field with frequencies of 8 and 50 Hz, as well as mechanical mixing effect with frequencies of 4.4 and 12 Hz (M ± SD, n = 6). *—statistically significant differences relative to unexposed samples (*t*-test, $p < 0.05$).

The impact of an alternating magnetic field with frequencies of 8 and 50 Hz, as well as mechanical stirring with frequencies of 4.4 and 12 Hz, on the concentration of O_2 in the colloid of IgG protein molecules was investigated (Figure 6b). It has been shown that the concentration of O_2 in H_2O and aqueous protein colloids changes under the influence of mechanical stirring with frequencies of 4.4 and 12 Hz; when exposed to an alternating magnetic field, a small statistically significant effect is observed at an IgG concentration of 0.1 mg/mL, although the trend is toward an increase in concentration when exposed to a magnetic field, and it is also noticeable for other IgG concentrations. In the case of mechanical action, a rather interesting effect is observed, namely, with mechanical action on

H_2O, the concentration of O_2 decreases, and when exposed to a protein colloid, it increases. It was previously shown that when an aqueous solution of sodium chloride saturated with atmospheric gases is subjected to mechanical action, a decrease in the concentration of O_2 is observed [68]. It has been shown that with mechanical impact on the protein colloid, the oxygen concentration, on the contrary, increases. This may probably be due to the absorption of protein molecules on the surface of nanometer-sized gas bubbles, which in turn leads to the retention of such gas bubbles inside the liquid [69]. At the same time, we cannot exclude other options conjoint with partial denaturation of molecules of proteins and the interaction of the hydrophobic core of such partially denatured molecules with gas molecules [70].

The impact of an alternating magnetic field with frequencies of 8 and 50 Hz, as well as mechanical stirring with frequencies of 4.4 and 12 Hz, on the redox potential of an aqueous protein colloid was investigated (Figure 6c). The redox potential of water and aqueous protein colloids tends to change in different directions. In water, there is a tendency to increase the value of the redox potential under all influences. In protein colloids, on the contrary, there is a tendency toward decreasing the redox potential under all influences. It is known that in H_2O, not concentrated aqueous solutions and electrolytes, the redox potential is largely determined by the concentration of O_2 dissolved in the liquid [71]. It is possible that changes in the concentration of O_2 dissolved in the liquid underlie the observed results.

The impact of an alternating magnetic field with frequencies of 8 and 50 Hz, as well as mechanical stirring with frequencies of 4.4 and 12 Hz, on the pH value of an aqueous colloid of proteins was investigated (Figure 6d). The pH of water and aqueous protein colloids does not change significantly. Minimal statistically significant differences are observed only when magnetic fields are applied to protein colloids (1 mg/mL). Simultaneously, there is a tendency to increase the pH value under mechanical influences and decrease the pH value when exposed to alternating magnetic fields.

The impact of an alternating magnetic field with frequencies of 8 and 50 Hz, as well as mechanical stirring with frequencies of 4.4 and 12 Hz, on the refractive index of an aqueous colloid of proteins was investigated (Figure 7a). RI of aqueous protein colloids does not undergo significant changes after physical exposure. The refractive index changes only by 3×10^{-6} when mechanical stirring with a frequency of 12 Hz is used. It is known that the RI of protein colloids increases during both protein hydrolysis [72] and denaturation [33]. It can be assumed that under the influences studied, no essential changes in protein globules are registered.

The impact of an alternating magnetic field with frequencies of 8 and 50 Hz, as well as mechanical stirring with frequencies of 4.4 and 12 Hz, on the fluorescence intensity of an aqueous colloid of IgG protein molecules (1 mg/mL) was studied (Figure 7b). It has been shown that the fluorescence intensity of aqueous protein colloids does not undergo significant changes after physical exposure. The only exception is mechanical stirring with a frequency of 12 Hz, in which case the fluorescence intensity changes by slightly more than 2%. It is known that the fluorescence intensity can increase upon partial melting of the protein globule, when the screening effect is removed [73]. In this sense, the fluorescence intensity data are consistent with the refractive index measurements of protein colloids.

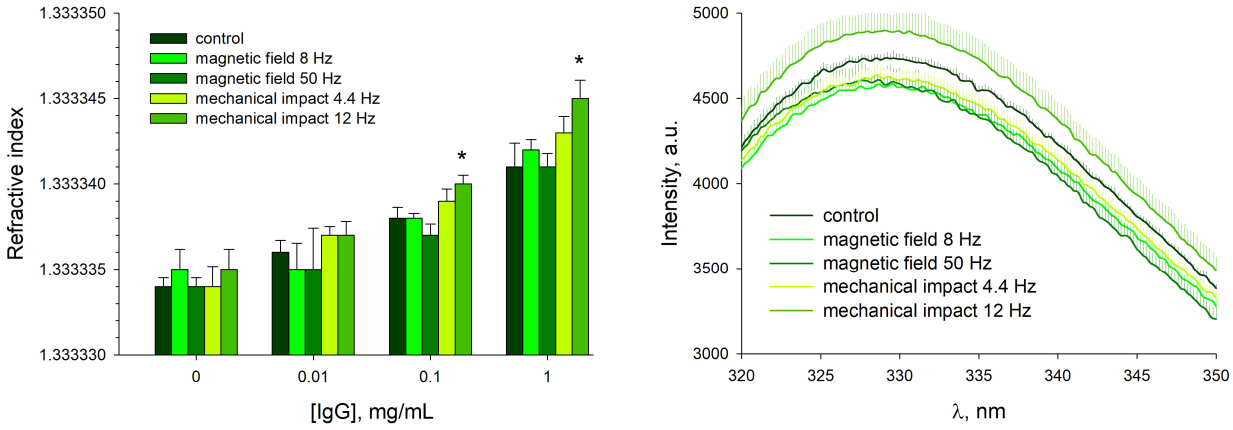

(**a**) (**b**)

Figure 7. Change in the refractive index (**a**) and fluorescence intensity (**b**) of aqueous colloid of IgG protein molecules after exposure to alternating magnetic field with frequencies of 8 and 50 Hz, as well as mechanical stirring with frequencies of 4.4 and 12 Hz (M ± SD, n = 6). The excitation wavelength when measuring fluorescence is 291 nm, and the protein concentration is 1 mg/mL. *—statistically significant difference relative to unexposed samples (*t*-test, $p < 0.05$).

There are several publications in which it is shown that magnetic fields with induction of the order of geomagnetic fields affect solutions [22,23]. The paper records the effects of water treated in a magnetic field, which was then used for watering plants, growing cell cultures, or drinking for animals and humans [74–77]. Such effects are often dependent on impurities in the water [78]. There are theoretical works that show that water protons can be targets of low-intensity magnetic fields [6]. The theories are based on the existence of metastable states of liquid water. Such states based on structural defects in water can be long-lived and be sensitive to MF effects [79].

Thus, it has been shown that when stirring in a turbulent flow, variations in the physicochemical properties of H_2O and aqueous colloids of the IgG protein are observed. Exposing the solutions described above to magnetic fields has no effect on water. However, in protein solutions, some parameters change. It is interesting to note that protein solutions are more susceptible to the action of alternating magnetic fields with a frequency of 8 Hz, and less subject to magnetic fields with a frequency of 50 Hz.

3.3. Duration of Changes in the Physicochemical Properties of Aqueous IgG Colloids after Exposure to a Magnetic Field and Mechanical Impact

After exposure to a magnetic field or mechanical stirring, measurements were taken as quickly as possible. It should be taken into account that moving the test tubes from the exposure installation to the measurement installation several meters away, pouring liquid into optical cuvettes, and moving the optical cuvette into the device takes some time (about half a minute). The measurement itself also has a duration from several seconds to several tens of seconds. It is known that the physical properties of water after the cessation of physical impact often return to control values quite quickly (from fractions of seconds to tens of seconds) [80–82]. In this case, changes in the secondary structure of protein molecules occur orders of magnitude slower due to steric restrictions. For example, after exposure to ionizing radiation, relaxation of long-lived radical forms of proteins occurs within several days [83]. In this work, the parameters of colloidal protein solutions were measured (not pure water and not dry protein molecules). In order to find out how long changes in the physicochemical properties of aqueous IgG colloids persist after exposure to a magnetic field and mechanical action, several series of experiments were carried out (Figure 8).

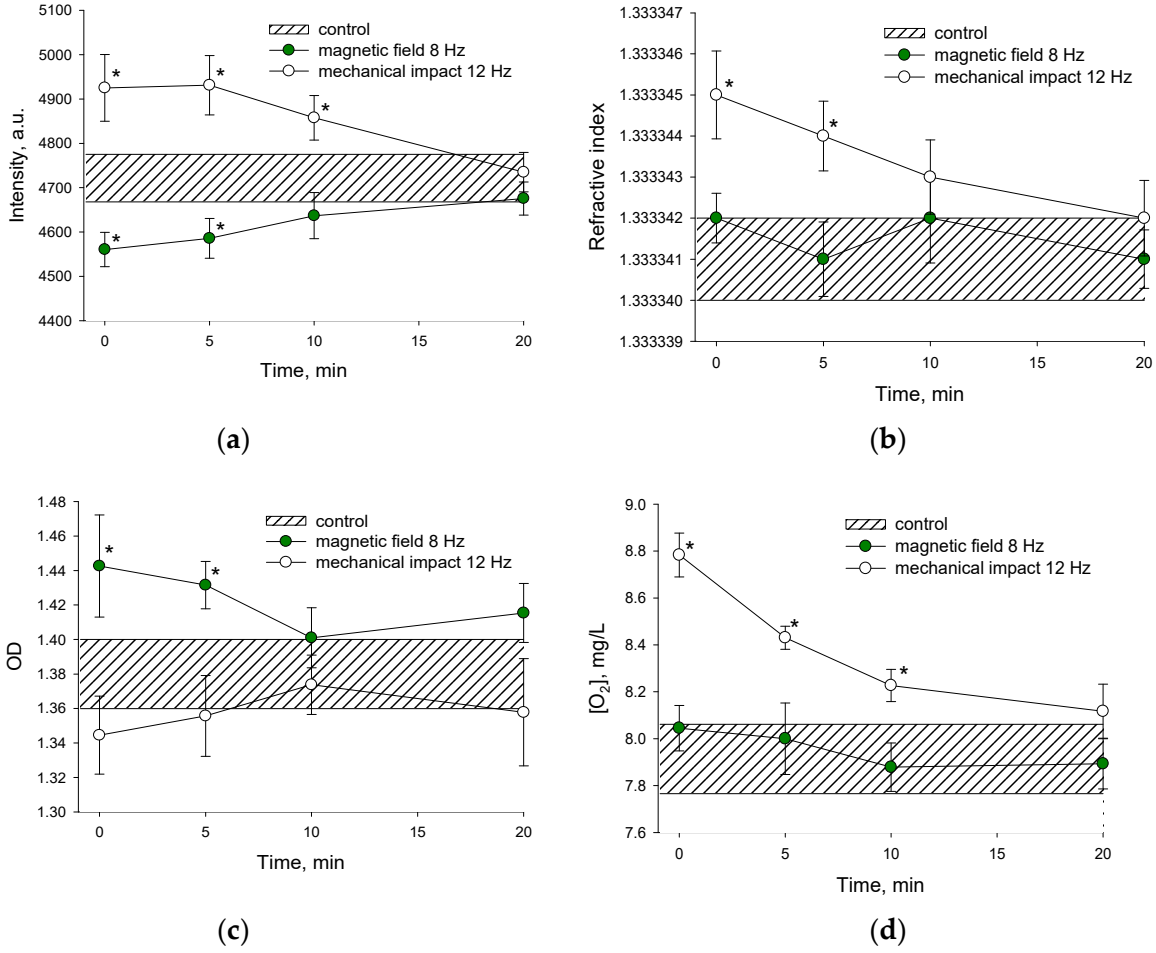

Figure 8. Duration of changes in the physicochemical properties of aqueous IgG colloids after exposure to a magnetic field (8 Hz) and mechanical impact (12 Hz). Changes in fluorescence intensity (**a**), refractive index (**b**), optical density (**c**), concentration of dissolved molecular oxygen (**d**). Protein concentration: 1 mg/mL. Time was counted from the beginning of parameter measurement. *—statistically significant differences relative to unexposed samples (*t*-test, $p < 0.05$).

The duration of changes in the fluorescence intensity of aqueous IgG colloids after exposure to a magnetic field (8 Hz) and mechanical action (12 Hz) was studied (Figure 8a). It was shown that immediately after exposure to a physical factor, maximum changes in the fluorescence intensity of IgG colloids were observed. When exposed to mechanical shaking, the fluorescence intensity increased by approximately 5%; when exposed to a magnetic field, the fluorescence intensity decreased by a similar amount. In general, the data obtained are consistent with the data presented in Figure 7b. When exposed to mechanical shaking, the increased fluorescence intensity compared to the control persisted for at least 10 min. When exposed to a magnetic field for at least 5 min, the luminescence intensity remained reduced compared to the control. A total of 20 min after exposure, the fluorescence intensity did not differ from control values.

The duration of change in the refractive index of aqueous IgG colloids after exposure to a magnetic field (8 Hz) and mechanical influence (12 Hz) was studied (Figure 8b). It has been shown that when exposed to a magnetic field for 20 min, no significant change in the refractive index of protein solutions is observed. When exposed to mechanical shaking, the refractive index increased by approximately 3×10^{-6}, which is consistent with the data presented in Figure 7a. The difference in the refractive index in the group subjected to mechanical action relative to the control is observed for at least 5 min.

The duration of change in the optical density of aqueous IgG colloids after exposure to a magnetic field (8 Hz) and mechanical action (12 Hz) was studied (Figure 8c). When

exposed to a magnetic field, the optical density increased by approximately 5%. When exposed to mechanical shaking, the optical density indicator at all studied exposure times was not statistically different from the control values, although it tended to decrease. In general, the data obtained are consistent with the data presented in Figure 5a. When exposed to a magnetic field, the increased optical density values compared to the control persisted for at least 5 min. A total of 10 min after exposure, the optical density of the colloids did not differ from the control values.

The duration of change in the concentration of dissolved molecular oxygen in aqueous IgG colloids after exposure to a magnetic field (8 Hz) and mechanical action (12 Hz) was studied (Figure 8d). It has been shown that when exposed to a magnetic field for 20 min, there is no significant change in the concentration of dissolved molecular oxygen in protein colloids. When exposed to mechanical shaking, the concentration of dissolved molecular oxygen increased by approximately 10%, which is consistent with the data presented in Figure 6b. When exposed to shaking for at least 10 min, the concentration of molecular oxygen dissolved in the aqueous IgG colloid remained increased compared to the control. A total of 20 min after exposure, the fluorescence intensity did not differ from control values. Thus, it has been shown that after the end of exposure to a magnetic field or mechanical stirring, the change in the properties of aqueous IgG colloids persists for at least 5–10 min.

3.4. Influence of Magnetic Field and Mechanical Action by Pipettingon the Physicochemical Properties of Water

In these experiments, an aqueous protein colloid and water were mixed in a ratio of 1/100, and in another, control series of experiments, water and water. This is due to the fact that our existing installation can mix solutions exactly in the current ratio. Obviously, with a single pipetting (mixing)of an aqueous protein colloid and water, a protein colloid is also obtained, albeit with a concentration one hundred times less (0.01 mg/mL). Therefore, we sequentially diluted the colloid 12 times in a row. As a result, we obtained a solution with an imaginary protein concentration of 10^{-24} mg/mL ("IgG (mix)"). Although the protein concentration in this solution is less than Avogadro's number, although a number of researchers believe that particles of the original substance may remain in such solutions [84,85]. For control, we carried out similar procedures and acted on a water–water mixture 12 times ("Water (mix)"). The resulting mixtures were exposed to an external magnetic field with frequencies of 8 and 50 Hz; no mechanical impact was used.

The impact of an alternating magnetic field with frequencies of 8 and 50 Hz on the electrical conductivity of H_2O was investigated (Figure 9a). It has been shown that the specific electrical conductivity of H_2O does not change under the impact of an alternating magnetic field with frequencies of 8 and 50 Hz. In the "Water (mix)" group, the specific electrical conductivity of water does not change significantly after the exposure of an external magnetic field with frequencies of 8 and 50 Hz. In the "IgG (mix)" group, the specific electrical conductivity of the sample decreases when exposed to an alternating magnetic field with a frequency of 50 Hz and in the absence of exposure to a magnetic field. When analyzing intergroup differences, it was shown that the control in the "IgG (mix)" group has almost two times lower specific electrical conductivity compared to the control in the "Water" and "Water (mix)" groups. Similar differences were found when comparing the specific electrical conductivity under the impact of an external magnetic field of 50 Hz in the "IgG (mix)" and "Water" groups.

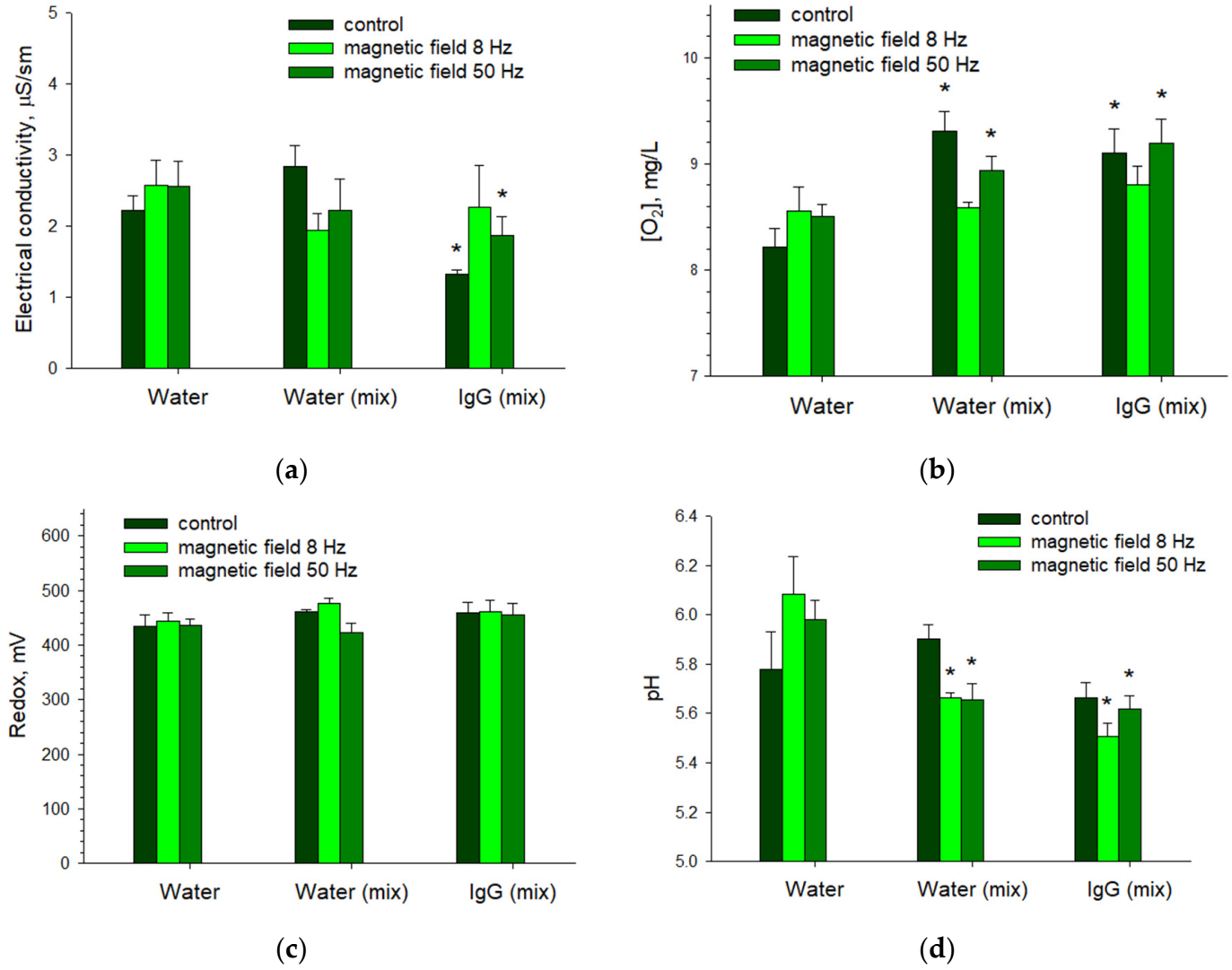

Figure 9. Changes in specific electrical conductivity (**a**), molecular oxygen concentration (**b**), oxidation–reduction potential (**c**), and pH (**d**) of water ("Water"), pipetted (mixed) water ("Water (mix)"), and a colloid of IgG protein molecules pipetted (mixed) with water ("IgG (mix)") after exposure to external magnetic field with frequencies of 8 and 50 Hz (M ± SD, n = 6). The IgG mix solution contains an imaginary amount of protein molecules (10^{-24} mg/mL). *—statistically significant differences relative to similar samples from the Water group (*t*-test, $p < 0.05$).

The impact of a magnetic field (8 and 50 Hz) on the concentration of O_2 dissolved in H_2O is shown in Figure 9b. It has been shown that O_2 concentration dissolved in H_2O does not change under the impact of an external magnetic field with frequencies of 8 and 50 Hz, although it tends to increase. In the "Water (mix)" group, the specific electrical conductivity of H_2O decreases under the influence of an alternating magnetic field (8 and 50 Hz). In the "IgG (mix)" group, the specific electrical conductivity of water does not change when exposed to an alternating magnetic field with frequencies of 8 and 50 Hz. When analyzing intergroup differences, it was shown that controls in the "Water (mix)" and "IgG (mix)" groups contained approximately 10% less dissolved molecular oxygen compared to the control in the "Water" group. Similar differences were established when comparing O_2 concentration under the impact of an alternating magnetic field with a frequency of 50 Hz.

The influence of an alternating magnetic field with frequencies of 8 and 50 Hz on the redox potential of water was investigated (Figure 9c). The redox potential does not change significantly under the impact of an alternating magnetic field with frequencies of 8 and 50 Hz in all groups. No intergroup differences were identified either.

Figure 9d shows how an external magnetic field with frequencies of 8 Hz and 50 Hz interferes with the pH value. It has been shown that the pH of water in the "Water" group does not change after exposure to an external magnetic field with frequencies of 8 and 50 Hz, although it tends to increase. In the "Water (mix)" group, the pH of H_2O decreases under the impact of an alternating magnetic field with frequencies of 8 and 50 Hz. In the "IgG (mix)" group, the pH of the water decreases only when exposed to an alternating magnetic field with a frequency of 8 Hz. When analyzing intergroup differences, it was shown that the controls in all groups had no significant differences. Wherein, significant differences were revealed when exposed to an alternating magnetic field with frequencies of 8 and 50 Hz in the "Water (mix)" and "IgG (mix)" groups compared to the "Water" group.

Thus, the study showed that aqueous solutions of IgG with a calculated concentration of 10^{-24} mg/mL are exposed to an alternating magnetic field, thereby exhibiting properties close to solutions of proteins of significant concentrations (which also respond to the influence of magnetic field), unlike water, which does not respond to the effects of external electromagnetic fields.

In general, the effects obtained have many similarities with hormesis and the manifesting dose effect. Let us recall that the phenomenon of a manifesting dose was discovered during the study of radiation hormesis several decades ago [86]. The essence of the phenomenon is as follows: when a biological object is exposed to a small dose of ionizing radiation, no changes in the object are detected. If after this the same object and an intact object are exposed to an electromagnetic field with a significantly higher intensity, then the changes in the intact object and in the object exposed to small doses of radiation will be significantly different. The second dose in this case became known as the manifesting dose [87]. Similar effects are observed for chemical substances, called the preconditioning effect, when a second administration of a drug can produce the effect of a small dose of the same or another drug. Various combinations of effects are known, for example, when a chemical effect is manifested by a physical one or vice versa. The preconditioning effect is known at the level of the organism [88,89], physiology [90,91], tissues [8,92], cells [93], and biological residues, liquids, aqueous colloids, and solutions [94,95], and, as shown in this study, in water.

Supplementary Materials: The following supporting information can be downloaded at: https://www.mdpi.com/article/10.3390/app132413055/s1, Each file in supplementary materials contains relevant data that correspond to a figure in the article.

Author Contributions: Conceptualization, E.I.N.; methodology, A.V.S. and V.I.P.; validation, V.E.R., V.P.K., V.A.K. and N.F.B.; formal analysis, N.A.S.; investigation, E.I.N., E.A.M., T.A.M., D.A.Z., A.V.S., E.V.S. and N.A.S.; resources, N.F.B.; writing—original draft preparation, E.I.N.; writing—review and editing, V.I.P. and N.F.B.; visualization, E.I.N. and E.A.M. All authors have read and agreed to the published version of the manuscript.

Funding: This work was supported with a grant of the Ministry of Science and Higher Education of the Russian Federation (075-15-2022-315) for the organization and development of a world-class research center "Photonics".

Institutional Review Board Statement: Not applicable.

Informed Consent Statement: Not applicable.

Data Availability Statement: Data is contained within the article and Supplementary Material.

Acknowledgments: The authors are grateful to the Center for Collective Use of the GPI RAS for the equipment provided.

Conflicts of Interest: The authors declare no conflict of interest.

Appendix A

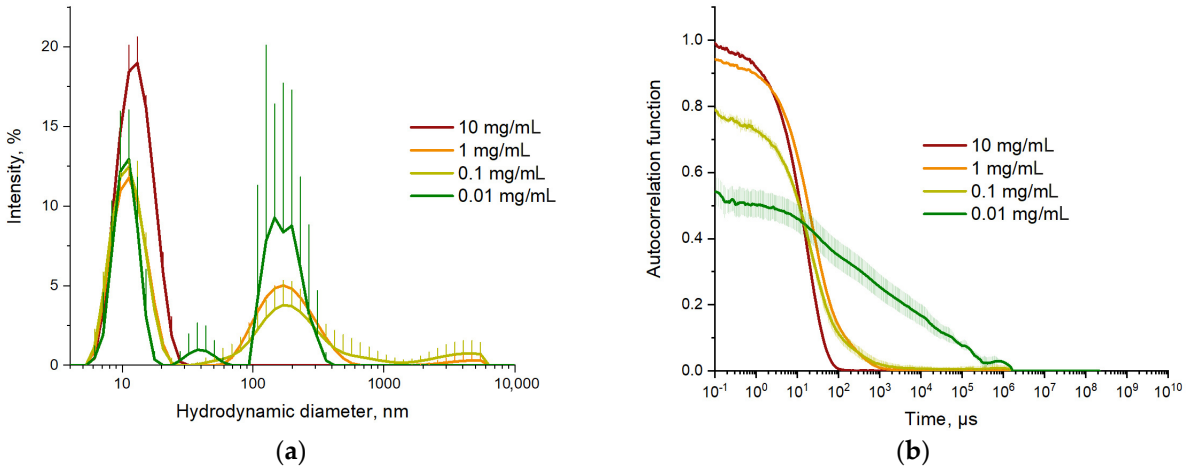

Figure A1. Hydrodynamic diameters of IgG solutions after filtration through a filter with an average pore size of about 200 nm (concentrations: 0.01–10 mg/mL), measured by DLS method (**a**) and autocorrelation functions obtained from these measurements (**b**).

References

1. Aszmann, O.C. The life and work of Theodore Schwann. *J. Reconstr. Microsurg.* **2000**, *16*, 291–295. [CrossRef]
2. Maksimenko, A.V. Approximation of new generation pharmacological enzyme researches to clinical practice. *Russ. Cardiol. Bull.* **2018**, *13*, 41–49. [CrossRef]
3. Caldevilla, R.; Morais, S.L.; Cruz, A.; Delerue-Matos, C.; Moreira, F.; Pacheco, J.G.; Santos, M.; Barroso, M.F. Electrochemical Chemically Based Sensors and Emerging Enzymatic Biosensors for Antidepressant Drug Detection: A Review. *Int. J. Mol. Sci.* **2023**, *24*, 8480. [CrossRef] [PubMed]
4. Ioannou, E.; Labrou, N.E. Development of Enzyme-Based Cosmeceuticals: Studies on the Proteolytic Activity of *Arthrospira platensis* and Its Efficient Incorporation in a Hydrogel Formulation. *Cosmetics* **2022**, *9*, 106. [CrossRef]
5. Hamid, B.; Bashir, Z.; Yatoo, A.M.; Mohiddin, F.; Majeed, N.; Bansal, M.; Poczai, P.; Almalki, W.H.; Sayyed, R.Z.; Shati, A.A.; et al. Cold-Active Enzymes and Their Potential Industrial Applications—A Review. *Molecules* **2022**, *27*, 5885. [CrossRef] [PubMed]
6. Castañeda Ruiz, A.J.; Shetab Boushehri, M.A.; Phan, T.; Carle, S.; Garidel, P.; Buske, J.; Lamprecht, A. Alternative Excipients for Protein Stabilization in Protein Therapeutics: Overcoming the Limitations of Polysorbates. *Pharmaceutics* **2022**, *14*, 2575. [CrossRef] [PubMed]
7. Mozhaeva, V.; Kudryavtsev, D.; Prokhorov, K.; Utkin, Y.; Garnov, S.V.; Kasheverov, I.; Tsetlin, V. Toxins' classification through Raman spectroscopy with principal component analysis. *Spectrochim. Acta Part A* **2022**, *278*, 121276. [CrossRef]
8. Mukhina, I.V.; Kazantsev, V.B.; Khaspeckov, L.G.; Zakharov, Y.N.; Vedunova, M.V.; Mitroshina, E.V.; Korotchenko, S.A.; Koryagina, E.A. Multielectrode Matrices—New Possibilities in Investigation of the Neuronal Network Plasticity. *Sovrem. Tehnol. V Med.* **2009**, *1*, 8–15.
9. Vedunova, M.B.; Mishchenko, T.A.; Mitroshina, E.V.; Ponomareva, N.V.; Yudintsev, A.V.; Generalova, A.N.; Deyev, S.M.; Mukhina, I.V.; Semyanov, A.V.; Zvyagin, A.V. Cytotoxic effects of upconversion nanoparticles in primary hippocampal cultures. *RSC Adv.* **2016**, *6*, 33656–33665. [CrossRef]
10. Jao, D.; Xue, Y.; Medina, J.; Hu, X. Protein-Based Drug-Delivery Materials. *Materials* **2017**, *10*, 517. [CrossRef]
11. Zhang, H.; Zhang, Y.; Zhang, C.; Yu, H.; Ma, Y.; Li, Z.; Shi, N. Recent Advances of Cell-Penetrating Peptides and Their Application as Vectors for Delivery of Peptide and Protein-Based Cargo Molecules. *Pharmaceutics* **2023**, *15*, 2093. [CrossRef] [PubMed]
12. Cui, J.; Wen, Z.; Zhang, W.; Wu, W. Recent Advances in Oral Peptide or Protein-Based Drug Liposomes. *Pharmaceuticals* **2022**, *15*, 1072. [CrossRef] [PubMed]
13. Mitroshina, E.V.; Mishchenko, T.A.; Usenko, A.V.; Epifanova, E.A.; Yarkov, R.S.; Gavrish, M.S.; Babaev, A.A.; Vedunova, M.V. AAV-Syn-BDNF-EGFP Virus Construct Exerts Neuroprotective Action on the Hippocampal Neural Network during Hypoxia In Vitro. *Int. J. Mol. Sci.* **2018**, *19*, 2295. [CrossRef] [PubMed]
14. State Pharmacopoeia of the Russian Federation XV Edition. General Pharmacopoeial Article "Biological Medicinal Products Obtained on the Basis of Gradual Technology" (OFS.1.7.00001). Available online: https://pharmacopoeia.regmed.ru/pharmacopoeia/izdanie-15/1/1-9/biologicheskie-lekarstvennye-preparaty-poluchennye-na-osnove-gradualnoy-tekhnologii/ (accessed on 6 December 2023).
15. Epstein, O. The Supramolecular Matrix Concept. *Symmetry* **2023**, *15*, 1914. [CrossRef]
16. Epstein, O. The Spatial Homeostasis Hypothesis. *Symmetry* **2018**, *10*, 103. [CrossRef]

17. Goncharov, R.G.; Rogov, K.A.; Temnov, A.A.; Novoselov, V.I.; Sharapov, M.G. Protective role of exogenous recombinant peroxiredoxin 6 under ischemia-reperfusion injury of kidney. *Cell Tissue Res.* **2019**, *378*, 319–332. [CrossRef] [PubMed]
18. Sharapov, M.; Novoselov, V.; Samygina, V.; Konarev, P.; Molochkov, A.; Sekirin, A.; Balkanov, A.; Gudkov, S. A chimeric recombinant protein with peroxidase and superoxide dismutase activities: Physico-chemical characterization and applicability to neutralize oxidative stress caused by ionizing radiation. *Biochem. Eng. J.* **2020**, *159*, 107603. [CrossRef]
19. Palomares, L.A.; Estrada-Moncada, S.; Ramírez, O.T. Production of Recombinant Proteins. In *Recombinant Gene Expression. Methods in Molecular Biology*; Balbás, P., Lorence, A., Eds.; Humana Press: Totowa, NJ, USA, 2004; Volume 267, pp. 15–51. [CrossRef]
20. Neurath, H.; Bull, H.B. The Surface Activity of Proteins. *Chem. Rev.* **1938**, *23*, 391–435. [CrossRef]
21. Chamorro, J.R.; McQueen, T.M.; Tran, T.T. Chemistry of Quantum Spin Liquids. *Chem. Rev.* **2021**, *121*, 2898–2934. [CrossRef]
22. Sarimov, R.M.; Serov, D.A.; Gudkov, S.V. Biological effects of magnetic storms and ELF magnetic fields. *Biology* **2023**, *12*, *accepted manuscript*.
23. Sarimov, R.M.; Serov, D.A.; Gudkov, S.V. Hypomagnetic conditions and their biological action (Review). *Biology* **2023**, *12*, *accepted manuscript*.
24. Baymler, I.V.; Gudkov, S.V.; Sarimov, R.M.; Simakin, A.V.; Shcherbakov, I.A. Concentration Dependences of Molecular Oxygen and Hydrogen in Aqueous Solutions. *Dokl. Phys.* **2020**, *65*, 5–7. [CrossRef]
25. Shcherbakov, I.A.; Baimler, I.V.; Lyakhov, G.A.; Mikhailova, G.N.; Pustovoy, V.I.; Sarimov, R.M.; Simakin, A.V.; Troitsky, A.V. Influence of a Constant Magnetic Field on Some Properties of Water Solutions. *Dokl. Phys.* **2020**, *65*, 273–275. [CrossRef]
26. Gudkov, S.V.; Simakin, A.V.; Bunkin, N.F.; Shafeev, G.A.; Astashev, M.E.; Glinushkin, A.P.; Grinberg, M.A.; Vodeneev, V.A. Development and application of photoconversion fluoropolymer films for greenhouses located at high or polar latitudes. *J. Photochem. Photobiol. B Biol.* **2020**, *213*, 112056. [CrossRef] [PubMed]
27. Shkirin, A.V.; Ignatenko, D.N.; Chirikov, S.N.; Vorobev, A.V. Application of Laser Polarimetric Scatterometry in the Study of Water-Based Multicomponent Bioorganic Systems on the Example of Cow Milk. *Phys. Wave Phenom.* **2022**, *30*, 186–195. [CrossRef]
28. Yanykin, D.V.; Astashev, M.E.; Khorobrykh, A.A.; Paskhin, M.O.; Serov, D.A.; Gudkov, S.V. Application of Fixed-Length Ultrasonic Interferometry to Determine the Kinetics of Light-/Heat-Induced Damage to Biological Membranes and Protein Complexes. *Inventions* **2022**, *7*, 87. [CrossRef]
29. Gudkov, S.V.; Simakin, A.V.; Sarimov, R.M.; Kurilov, A.D.; Chausov, D.N. Novel Biocompatible with Animal Cells Composite Material Based on Organosilicon Polymers and Fullerenes with Light-Induced Bacteriostatic Properties. *Nanomaterials* **2021**, *11*, 2804. [CrossRef] [PubMed]
30. Astashev, M.E.; Serov, D.A.; Sarimov, R.M.; Gudkov, S.V. Influence of the Vibration Impact Mode on the Spontaneous Chemiluminescence of Aqueous Protein Solutions. *Phys. Wave Phenom.* **2023**, *31*, 189–199. [CrossRef]
31. Masi, A.; Cicchi, R.; Carloni, A.; Pavone, F.S.; Arcangeli, A. Optical Methods in the Study of Protein-Protein Interactions. In *Integrins and Ion Channels. Advances in Experimental Medicine and Biology*; Becchetti, A., Arcangeli, A., Eds.; Springer: New York, NY, USA, 2010; Volume 674. [CrossRef]
32. Sarimov, R.M.; Binhi, V.N.; Matveeva, T.A.; Penkov, N.V.; Gudkov, S.V. Unfolding and Aggregation of Lysozyme under the Combined Action of Dithiothreitol and Guanidine Hydrochloride: Optical Studies. *Int. J. Mol. Sci.* **2021**, *22*, 2710. [CrossRef]
33. Sarimov, R.M.; Nagaev, E.I.; Matveyeva, T.A.; Binhi, V.N.; Burmistrov, D.E.; Serov, D.A.; Astashev, M.E.; Simakin, A.V.; Uvarov, O.V.; Khabatova, V.V.; et al. Investigation of Aggregation and Disaggregation of Self-Assembling Nano-Sized Clusters Consisting of Individual Iron Oxide Nanoparticles upon Interaction with HEWL Protein Molecules. *Nanomaterials* **2022**, *12*, 3960. [CrossRef]
34. Tan, Y.H.; Liu, M.; Nolting, B.; Go, J.G.; Gervay-Hague, J.; Liu, G. A Nanoengineering Approach for Investigation and Regulation of Protein Immobilization. *ACS Nano* **2008**, *2*, 2374–2384. [CrossRef] [PubMed]
35. Wong, K.S.; Chew, N.S.L.; Low, M.; Tan, M.K. Plasma-Activated Water: Physicochemical Properties, Generation Techniques, and Applications. *Processes* **2023**, *11*, 2213. [CrossRef]
36. Bunkin, N.F.; Bunkin, F.V. Bubston structure of water and electrolyte aqueous solutions. *Phys. Uspekhi* **2016**, *59*, 846. [CrossRef]
37. Zhou, Y.; Han, Z.; He, C.; Feng, Q.; Wang, K.; Wang, Y.; Luo, N.; Dodbiba, G.; Wei, Y.; Otsuki, A.; et al. Long-Term Stability of Different Kinds of Gas Nanobubbles in Deionized and Salt Water. *Materials* **2021**, *14*, 1808. [CrossRef] [PubMed]
38. Yadav, S.; Shire, S.J.; Kalonia, D.S. Factors Affecting the Viscosity in High Concentration Solutions of Different Monoclonal Antibodies. *J. Pharm. Sci.* **2010**, *99*, 4812–4829. [CrossRef] [PubMed]
39. Cheng, W.; Joshi, S.B.; Jain, N.K.; He, F.; Kerwin, B.A.; Volkin, D.V.; Middaugh, C.R. Linking the Solution Viscosity of an IgG2 Monoclonal Antibody to Its Structure as a Function of pH and Temperature. *J. Pharm. Sci.* **2013**, *102*, 4291–4304. [CrossRef] [PubMed]
40. Yadav, S.; Liu, J.; Shire, S.J.; Kalonia, D.S. Specific interactions in high concentration antibody solutions resulting in high viscosity. *J. Pharm. Sci.* **2010**, *99*, 1152–1168. [CrossRef]
41. Salinas, B.A.; Sathish, H.A.; Bishop, S.M.; Harn, N.; Carpenter, J.F.; Randolph, T.W. Understanding and Modulating Opalescence and Viscosity in a Monoclonal Antibody Formulation. *J. Pharm. Sci.* **2010**, *99*, 82–93. [CrossRef]
42. Zidar, M.; Rozman, P.; Belko-Parkel, K.; Ravnik, M. Control of viscosity in biopharmaceutical protein formulations. *J. Colloid Interface Sci.* **2020**, *580*, 308–317. [CrossRef]
43. Mosca, I.; Pounot, K.; Beck, C.; Colin, L.; Matsarskaia, O.; Grapentin, C.; Seydel, T.; Schreiber, F. Biophysical Determinants for the Viscosity of Concentrated Monoclonal Antibody Solutions. *Mol. Pharm.* **2023**, *20*, 4698–4713. [CrossRef]

44. Prass, T.M.; Garidel, P.; Blech, M.; Schäfer, L.V. Viscosity Prediction of High-Concentration Antibody Solutions with Atomistic Simulations. *J. Chem. Inf. Model.* **2023**, *63*, 6129–6140. [CrossRef] [PubMed]
45. Zhang, Z.; Liu, Y. Recent progresses of understanding the viscosity of concentrated protein solutions. *Curr. Opin. Chem. Eng.* **2017**, *16*, 48–55. [CrossRef]
46. Nagaev, E.I.; Baimler, I.V.; Baryshev, A.S.; Astashev, M.E.; Gudkov, S.V. Effect of Laser-Induced Optical Breakdown on the Structure of Bsa Molecules in Aqueous Solutions: An Optical Study. *Molecules* **2022**, *27*, 6752. [CrossRef] [PubMed]
47. Simakin, A.V.; Sarimov, R.M.; Smirnova, V.V.; Astashev, M.E.; Serov, D.A.; Yanykin, D.V.; Chausov, D.N.; Shkirin, A.V.; Uvarov, O.V.; Rotanov, E.; et al. New Structural Nanocomposite Based on PLGA and Al_2O_3 NPs as a Balance between Antibacterial Activity and Biocompatibility with Eukaryotic Cells. *J. Compos. Sci.* **2022**, *6*, 298. [CrossRef]
48. Zhao, H.; Brown, P.H.; Schuck, P. On the distribution of protein refractive index increments. *Biophys. J.* **2011**, *100*, 2309–2317. [CrossRef]
49. Ball, V.; Ramsden, J.J. Buffer dependence of refractive index increments of protein solutions. *Biopolymers* **1998**, *46*, 489–492. [CrossRef]
50. Carlson, T. The diffusion of oxygen in water. *J. Am. Chem. Soc.* **1911**, *33*, 1027–1032. [CrossRef]
51. Abraham, G.N. Human triclonal anti-IgG gammopathy. I. Iso-electric focusing characteristics of the IgG, IgA and IgM anti-IgG and their heavy and light chains. *Immunology* **1978**, *35*, 429–436.
52. Abdelraheem, E.M.M.; Busch, H.; Hanefeld, U.; Tonin, F. Biocatalysis explained: From pharmaceutical to bulk chemical production. *React. Chem. Eng.* **2019**, *4*, 1878–1894. [CrossRef]
53. Besser, B.P. Synopsis of the historical development of Schumann resonances. *Radio Sci.* **2007**, *42*, 20. [CrossRef]
54. Matveeva, T.A.; Baimler, I.V.; Artemiev, K.V.; Gorudko, I.V.; Sarimov, R.M. Laser Optical Breakdown Modified Physical Properties of Lysozyme in Aqueous Solution. *Opera Medica Physiol.* **2022**, *9*, 126–136. [CrossRef]
55. Yu, Z.; Reid, J.C.; Yang, Y.P. Utilizing dynamic light scattering as a process analytical technology for protein folding and aggregation monitoring in vaccine manufacturing. *J. Pharm. Sci.* **2013**, *102*, 4284–4290. [CrossRef] [PubMed]
56. Bobylev, A.G.; Penkov, N.V.; Troshin, P.A.; Gudkov, S.V. The effect of dilution on the aggregation of polycarboxylated C_{60} fullerene nanoparticles. *Biophysics* **2015**, *60*, 30–34. [CrossRef]
57. Biswas, B.; Muttathukattil, A.N.; Reddy, G.; Singh, P.C. Contrasting Effects of Guanidinium Chloride and Urea on the Activity and Unfolding of Lysozyme. *Acs Omega* **2018**, *3*, 14119–14126. [CrossRef] [PubMed]
58. Wu, K.; Yu, L.; Zheng, X.; Wang, Y.; Feng, Y.; Tu, L.; Wang, J.P. Viscosity effect on the brownian relaxation based detection for immunoassay applications. *IEEE Eng. Med. Biol. Soc.* **2014**, 2769–2772. [CrossRef]
59. Jyoti, D.; Gordon-Wylie, S.W.; Reeves, D.B.; Paulsen, K.D.; Weaver, J.B. Distinguishing Nanoparticle Aggregation from Viscosity Changes in MPS/MSB Detection of Biomarkers. *Sensors* **2022**, *22*, 6690. [CrossRef]
60. Astashev, M.E.; Belosludtsev, K.N.; Kharakoz, D.P. Method for digital measurement of phase-frequency characteristics for a fixed-length ultrasonic spectrometer. *Acoust. Phys.* **2014**, *60*, 335–341. [CrossRef]
61. Shcherbakov, I.A. Influence of External Impacts on the Properties of Aqueous Solutions. *Phys. Wave Phenom.* **2021**, *29*, 89–93. [CrossRef]
62. Shcherbakov, I.A. Current Trends in the Studies of Aqueous Solutions. *Phys. Wave Phenom.* **2022**, *30*, 129–134. [CrossRef]
63. Bruskov, V.I.; Karmanova, E.E.; Chernikov, A.V.; Usacheva, A.M.; Ivanov, V.E.; Emel'yanenko, V.I. Formation of Hydrated Electrons in Water under Thermal Electromagnetic Exposure. *Phys. Wave Phenom.* **2021**, *29*, 94–97. [CrossRef]
64. Gudkov, S.V.; Penkov, N.V.; Baimler, I.V.; Lyakhov, G.A.; Pustovoy, V.I.; Simakin, A.V.; Sarimov, R.M.; Scherbakov, I.A. Effect of Mechanical Shaking on the Physicochemical Properties of Aqueous Solutions. *Int. J. Mol. Sci.* **2020**, *21*, 8033. [CrossRef]
65. Chernikov, A.V.; Gudkov, S.V.; Shtarkman, I.N.; Bruskov, V.I. Oxygen effect in heat-mediated damage to DNA. *Biofizika* **2007**, *52*, 244–251. [PubMed]
66. Bruskov, V.I.; Chernikov, A.V.; Gudkov, S.V.; Masalimov, Z.K. Thermal Activation of the Reducing Properties of Seawater Anions. *Biofizika* **2003**, *48*, 1022–1029. [PubMed]
67. Chen, B.; Xia, Y.; He, R.; Sang, H.; Zhang, W.; Li, J.; Chen, L.; Wang, P.; Guo, S.; Yin, Y.; et al. Water-solid contact electrification causes hydrogen peroxide production from hydroxyl radical recombination in sprayed microdroplets. *Proc. Natl. Acad. Sci. USA* **2022**, *119*, e2209056119. [CrossRef] [PubMed]
68. Sarimov, R.M.; Simakin, A.V.; Matveeva, T.A.; Lyakhov, G.A.; Pustovoy, V.I.; Troitskii, A.V.; Shcherbakov, I.A. Influence of Magnetic Fields with Induction of 7 T on Physical and Chemical Properties of Aqueous NaCl Solutions. *Appl. Sci.* **2021**, *11*, 11466. [CrossRef]
69. Bunkin, N.F.; Shkirin, A.V.; Ninham, B.W.; Chirikov, S.N.; Chaikov, L.L.; Penkov, N.V.; Kozlov, V.A.; Gudkov, S.V. Shaking-induced aggregation and flotation in immunoglobulin dispersions: Differences between water and water-ethanol mixtures. *ACS Omega* **2020**, *5*, 14689–14701. [CrossRef] [PubMed]
70. Privalov, P.L.; Gill, S.J. Stability of Protein Structure and Hydrophobic Interaction. *Adv. Protein Chem.* **1988**, *39*, 191–234. [CrossRef] [PubMed]
71. Goncharuk, V.V.; Bagrii, V.A.; Mel'nik, L.A.; Chebotareva, R.D.; Bashtan, S.Y. The use of redox potential in water treatment processes. *J. Water Chem. Technol.* **2010**, *32*, 1–9. [CrossRef]
72. Sarimov, R.M.; Matveyeva, T.A.; Binhi, V.N. Laser interferometry of the hydrolytic changes in protein solutions: The refractive index and hydration shells. *J. Biol. Phys.* **2018**, *44*, 345–360. [CrossRef]

73. Ptitsyn, O.B. Protein folding: Hypotheses and experiments. *J. Protein Chem.* **1987**, *6*, 273–293. [CrossRef]
74. Pandey, S.; Garg, T.; Singh, K.; Rai, S. Effect of magnetically induced water structure on the oestrous cycles of albino female mice Musmusculus. *Electro-Magnetobiol.* **1996**, *15*, 133–140. [CrossRef]
75. Rai, S.; Garg, T.; Vashistha, H. Possible Effect of Magnetically Induced Water Structures on Photosynthetic Electron Transport Chains of a Green Alga Chlorella Vulgarts. *Electro-Magnetobiol.* **1996**, *15*, 49–55. [CrossRef]
76. Devyatkov, N.D.; Kislov, V.Y.; Kislov, V.V.; Kolesov, V.V.; Smirnov, V.F.; Chigin, E.P. Detection of the effect of normalisation of the functional state of human internal organs under the influence of water activated by millimetre radiation. *Millimetre Waves Biol. Med.* **1996**, *8*, 65–68.
77. Ružič, R.; Jerman, I. Influence of Ca^{2+} in biological effects of direct and indirect ELF magnetic field stimulation. *Electro-Magnetobiol.* **1998**, *17*, 205–216.
78. Colic, M.; Morse, D. Mechanism of the long-term effects of electromagnetic radiation on solutions and suspended colloids. *Langmuir* **1998**, *14*, 783–787. [CrossRef]
79. Binhi, V.N. *Magnetobiology: Underlying Physical Problems*; Academic Press: San Diego, CA, USA, 2002.
80. Keene, J.P. Absorption spectra in irradiated water and some solutions. Part II. Optical absorptions in irradiated water. *Nature* **1963**, *197*, 47–48. [CrossRef]
81. Patil, P.N.; Sawant, D.V.; Deshmukh, R.N. Physico-chemical parameters for testing of water—A review. *Int. J. Environ. Sci.* **2012**, *3*, 1194–1207.
82. Gonella, G.; Backus, E.H.G.; Nagata, Y.; Bonthuis, D.J.; Loche, P.; Schlaich, A.; Netz, R.R.; Kühnle, A.; McCrum, I.T.; Koper, M.T.M.; et al. Water at charged interfaces. *Nat. Rev. Chem.* **2021**, *5*, 466–485. [CrossRef]
83. Wang, H.; Liu, R.; Tu, T.; Xie, L.; Sheng, K.; Chen, Y.; Tang, X. Properties of Radicals Formed by the Irradiation of Wool Fibers. *J. Radiat. Res.* **2004**, *45*, 77–81. [CrossRef]
84. Chikramane, P.S.; Kalita, D.; Suresh, A.K.; Kane, S.G.; Bellare, J.R. Why extreme dilutions reach non-zero asymptotes: A nanoparticulate hypothesis based on froth flotation. *Langmuir* **2012**, *28*, 15864–15875. [CrossRef]
85. Tytik, D.L.; Souvorova, O.V.; Kuz'min, V.I.; Revina, A.A. Relaxation of Aqueous Solutions in Successive Dilutions of Antibodies to S100 Protein According to Luminescence Data. *Phys. Wave Phenom.* **2023**, *31*, 200–205. [CrossRef]
86. Calabrese, E.J.; Baldwin, L.A. Hormesis: The Dose-Response Revolution. *Annu. Rev. Pharmacol. Toxicol.* **2023**, *43*, 175–197. [CrossRef] [PubMed]
87. Zaichkina, S.I.; Rozanova, O.M.; Dyukina, A.R.; Simonova, N.B.; Romanchenko, S.P.; Sorokina, S.S.; Aptikaeva, G.F.; Yusupov, V.I. Influence of low-dose-rate red and near-infrared radiations on the level of reactive oxygen species, the genetic apparatus and the tumor growth in mice in vivo. *Biophysics* **2013**, *58*, 712–717. [CrossRef]
88. Xu, H.; Takashi, E.; Liang, J.; Chen, Y.; Yuan, Y.; Fan, J. Effect of Heat Shock Preconditioning on Pressure Injury Prevention via Hsp27 Upregulation in Rat Models. *Int. J. Mol. Sci.* **2022**, *23*, 8955. [CrossRef]
89. Delatorre-Castillo, J.P.; Delatorre-Herrera, J.; Lay, K.S.; Arenas-Charlín, J.; Sepúlveda-Soto, I.; Cardemil, L.; Ostria-Gallardo, E. Preconditioning to Water Deficit Helps *Aloe vera* to Overcome Long-Term Drought during the Driest Season of Atacama Desert. *Plants* **2022**, *11*, 1523. [CrossRef] [PubMed]
90. Leurcharusmee, P.; Sawaddiruk, P.; Punjasawadwong, Y.; Sugundhavesa, N.; Klunklin, K.; Tongprasert, S.; Sitilertpisan, P.; Jaiwongkam, T.; Apaijai, N.; Chattipakorn, N.; et al. CoenzymeQ10 and Ischemic Preconditioning Potentially Prevent Tourniquet-Induced Ischemia/Reperfusion in Knee Arthroplasty, but Combined Pretreatment Possibly Neutralizes Their Beneficial Effects. *Antioxidants* **2022**, *11*, 419. [CrossRef] [PubMed]
91. Xie, R.; Zeng, X.; Yan, H.; Huang, X.; Deng, C. Effects and Mechanisms of Exosomes from Different Sources in Cerebral Ischemia. *Cells* **2022**, *11*, 3623. [CrossRef]
92. Belity, T.; Horowitz, M.; Hoffman, J.R.; Epstein, Y.; Bruchim, Y.; Todder, D.; Cohen, H. Heat-Stress Preconditioning Attenuates Behavioral Responses to Psychological Stress: The Role of HSP-70 in Modulating Stress Responses. *Int. J. Mol. Sci.* **2022**, *23*, 4129. [CrossRef]
93. Cheng, Y.-H.; Chen, K.-H.; Sung, Y.-T.; Yang, C.-C.; Chien, C.-T. Intrarenal Arterial Transplantation of Dexmedetomidine Preconditioning Adipose Stem-Cell-Derived Microvesicles Confers Further Therapeutic Potential to Attenuate Renal Ischemia/Reperfusion Injury through miR-122-5p/Erythropoietin/Apoptosis Axis. *Antioxidants* **2022**, *11*, 1702. [CrossRef]
94. Ogundele, O.M.; Gbashi, S.; Oyeyinka, S.A.; Kayitesi, E.; Adebo, O.A. Optimization of Infrared Heating Conditions for Precooked Cowpea Production Using Response Surface Methodology. *Molecules* **2021**, *26*, 6137. [CrossRef]
95. Shishkina, A.V.; Ksenofontov, A.A.; Penkov, N.V.; Vener, M.V. Diclofenac Ion Hydration: Experimental and Theoretical Search for Anion Pairs. *Molecules* **2022**, *27*, 3350. [CrossRef] [PubMed]